TRANSFORMATION OPTICS AND TOPOLOGICAL PHASES OF CHIRAL PHOTONIC CRYSTALS

LAU Ting Wai

MPhil

The Hong Kong Polytechnic University

2021

The Hong Kong Polytechnic University

Department of Applied Physics

Transformation Optics and Topological Phases of Chiral Photonic Crystals

LAU Ting Wai

A thesis submitted in partial fulfilment of the requirements

for the degree of Master of Philosophy

August 2020

Certificate of originality

I hereby declare that this thesis is my own work and that, to the best of my knowledge and belief, it reproduces no material previously published or written, nor material that has been accepted for the award of any other degree or diploma, except where due acknowledgement has been made in the text.

_____(Signed)

LAU, Ting Wai (Name of student)

Abstract

The topology of chiral materials is attractive because a wider parameter space can be provided by the coupling of electric and magnetic fields in their constitutive relations. Parity inversion symmetry is already broken without applying external magnetic fields due to left-handed and right-handed circular polarization of optical activity; however, the time reversal symmetries can still be preserved. Optical activities has been gradually taken into consideration when developing the topological theories of bi-anisotropic materials. In this study, the techniques of transformation optics have been used to design one-dimensional chiral photonic crystals. Transformation optics is a theory based on the invariance of Maxwell's equations under coordinate transformation. Due to the flexibility of Jacobian matrix, the trajectory of a light beam can be controlled so that some "unrealistic" phenomena in conventional view can be easily achieved, for example, illusion optics. However, coordinate transformation is not valid to predict electromagnetic properties in bi-anisotropic medium via simple anisotropic medium since the constitutive relations of the media are different. Other transformation method is also investigated such that there exists a conformal mapping between two spaces. Instead of the trajectory, optical activity attributed to chirality can be controlled owing to the flexibility of the transformation

matrix. The designed chiral materials will act as a unit cell of a photonic crystal such that a chiral photonic crystal can be constructed. Topological features, Zak phases and topological edge states, of the designed chiral photonic crystals are examined. The eigenmodes, TE and TM modes, are no longer degenerated because of anisotropy and existence of chirality. Zak phases calculated by these coupled eigenstates are briefly discussed. With choosing suitable electromagnetic tensors, two independent modes can be decoupled such that the topological theories developed from simple isotropic layered photonic crystals can be totally applied.

Acknowledgement

I would like to take this opportunity to express my sincere gratitude to my supervisors Dr. K. H. Fung for valuable advice and guidance. Advice, ideas and supports have been given on the research. I would also like to thank my colleagues, research group-mates and all the people who helped me in my post graduate study.

Contents

List of Figures

List of Tables

Chapter 1

Introduction

1.1 Overview and objectives

The theory of transformation optics has been raised up since two independent studies proposed by Pendry *et. al.* [1] and Leonhardt [2] in 2006. This theory can provide more information on the electromagnetic parameters for achieving specific physical phenomena [3]. On the basis of the invariances of Maxwell's equations and Helmholz equation under coordinate transformation, the electromagnetic (EM) waves and electromagnetic tenors in the original and transformed spaces have a one-to-one mapping method, which is called conformal or quasi-conformal mapping [2–7]. The idea is similar to general relativity [8]. The wave properties in flat space will be used to predict the properties in curve spaces. Rather than first considering the structure of the materials, the trajectory of EM waves can be easily controlled by the flexibility of the Jacobian matrix; therefore, some physical phenomena being hardly achieved in conventional ways can be easily overcome [1–7]. Famous examples

are matematerials, illusion optics [2–4], polarization splitters [5], extreme plasmonics [6] and antenna [7]. Although recent studies are mainly focusing on controlling the path of light to achieve particular phenomena, the techniques of transformation optics are also able to transform simple anisotropic media to bi-anisotropic media. Bi-anisotropic materials are attractive because optical activities can occur in bi-anisotropic medium without applying external magnetic fields [9]. Because of the differences of the constitutive relations between two media, other transformation methods should be considered instead of coordinate transformation [8]. In this thesis, the transformation between one-dimensional (1D) simple anisotropic media and 1D anisotropic media with isotropic chirality is investigated. Instead of the trajectory, optical activity can be controlled owing to the flexibility of the transformation matrix; on the other hand, the theories developed from 1D simple anisotropic materials can be totally applied since there is a mapping between simple and chiral media.

Transformation optics can achieve some physical phenomena, and some properties can still be retained after continuous spatial deformation, for example, topological features [10]. Topological photonics becomes attractive since Haldane and Raghu [11] had transformed the ideas from quantum electronic systems to photonic crystals in 2005 [10]. It has been gradually confirmed by the recent experimental results [12–16]. The analogy of topological system between quantum electric system and photonic system is widely discussed in recent studies [10, 17]. Due to the coupling of electric and magnetic fields, bi-anisotropic materials can provide a wider parameter space for the realization of different topological phases compared to simple anisotropic materials [10, 18]. Furthermore, parity inversion symmetry of chiral

materials is broken due to natural optical activities [9, 10, 19–21], whereas the time-reversal symmetry can still be preserved [10, 19]. In some studies, left-handed and right-handed circular polarization (LCP and RCP) of optical activities contributed by chirality ("spin" of photons) is taken into consideration, and chiral matematerials are used to design photonic topological insulators [18, 19]. Non-trivial topological phases of chiral metamaterials have been theoretically demonstrated in recent studies [21, 22]. In this study, the concept of "spin" of photons is not required and only the topological theories of simple isotropic binary photonic crystals are applied. By treating the designed 1D chiral material as a unit cell of a photonic crystal, a 1D chiral photonic crystal can be constructed. Zak phases and topological edge states of the designed chiral photonic crystals are investigated.

In chapter 1, some fundamental concepts of chiral materials, ideas of transformation optics and topological theories of photonic systems are reviewed. In chapter 2, the details of the transformation between 1D simple anisotropic medium and 1D anisotropic medium with isotropic chirality are discussed. The band structures of the designed chiral photonic crystals are also investigated. Zak phases of the chiral photonic crystals and the topological properties are examined in chapter 3.

1.2 Reviews on chiral materials

Chiral materials are composed of the particles, especially molecules, which cannot superimposed on their mirror images (enantiomer) [23, 24]. The discovery of optical actvities caused by chirality can be traced back to early 19th century [9, 23]. In 1811, Arago discovered rotatory dispersion occurred in quartz crystals [9]. Few

Table 1.1: Classification of bi-anisotropic media. [9]

	$\boldsymbol{\kappa} = \mathbf{0}$	$\boldsymbol{\kappa} \neq \mathbf{0}$
$\boldsymbol{\chi} = \mathbf{0}$	Simple anisotropic medium	Anisotropic chiral medium
$\boldsymbol{\chi} \neq \mathbf{0}$	Tellegen medium	General bi-anisotropic medium

years later, Biot proposed the optical rotation should be attributed to the molecules rather than their aggregates in solid state since optical rotation can occur in liquid and gases [9, 23]. This phenomenon is named to be natural optical activity and the materials which can induce this effect are called chiral materials. Before reviewing the constitutive relations, we should clarify the distinction between natural and magnetic optical activities. Natural optical activity is caused by the chiral molecules and the phenomenon is reciprocal. For instance, by assuming the position of the observer is unchanged, if the direction of optical rotation is anticlockwise , the rotation will be clockwise when the light is propagating from the opposite direction. In contrast, magnetic optical activity (or called Faradays rotation) is non-reciprocal, which is induced via applying external magnetic field to particular achiral media so that the media become anisotropic. More details of the differences can be found in Refs. [24, 25].

Electromagnetic waves in materials are governed by the Maxwell's equations and the constitutive relations. The constitutive relations of general bi-anisotropic media can be written as [26]

$$\mathbf{D} = \varepsilon_0 \boldsymbol{\varepsilon} \mathbf{E} - \sqrt{\varepsilon_0 \mu_0}\,(\boldsymbol{\chi}^T - i\boldsymbol{\kappa}^T)\mathbf{H},\ \mathbf{B} = \sqrt{\varepsilon_0 \mu_0}\,(\boldsymbol{\chi} + i\boldsymbol{\kappa})\mathbf{E} + \mu_0 \boldsymbol{\mu} \mathbf{H}, \tag{1.1}$$

where $\mathbf{E}$ and $\mathbf{B}$ are electric and magnetic fields respectively; also, $\mathbf{D}$ and $\mathbf{H}$ are

macroscopic electromagnetic fields. $\boldsymbol{\varepsilon}$ and $\boldsymbol{\mu}$ are relative dielectric permittivity and magnetic permeability tensors. ε_0 and μ_0 are permittivity and permeability in free space. The magneto-electric material tensors $\boldsymbol{\chi}$ and $\boldsymbol{\kappa}$ are called non-reciprocity and chirality tensors respectively. Noted that the magneto-electric material tensors are dimensionless and they are pesudotensors [27]. i.e.,

$$\mathcal{P}\{\boldsymbol{\chi}(\mathbf{r})\} = -\boldsymbol{\chi}(-\mathbf{r}), \;\; \mathcal{P}\{\boldsymbol{\kappa}(\mathbf{r})\} = -\boldsymbol{\kappa}(-\mathbf{r}), \tag{1.2}$$

where $\mathcal{P}$ is spatial–inversion operator. Table 1.1 shows the classification of bi-anisotropic media according to the coupling of $\boldsymbol{\chi}$ and $\boldsymbol{\kappa}$. In this study, non-reciprocal properties of materials, magneto-electric effects, are not included and thereby $\boldsymbol{\chi}$ is assumed to be $\mathbf{0}$. Although chiral materials are not uncommon in nature, the values of chirality parameters of nature materials are usually small [9, 24]; nevertheless, strong chiral effects can be produced by resonant or artificial fabrication [9, 24, 28]. According to the properties of matrices, chirality tensor can be decomposed in the form [26]:

$$\boldsymbol{\kappa} = \kappa\mathbf{I} + \mathbf{N} + \mathbf{J}, \tag{1.3}$$

where $\mathbf{I}$, $\mathbf{N}$ and $\mathbf{J}$ are identity, symmetric and anti-symmetric matrices respectively. Hence, as shown in Table 1.2, chiral media can be further classified into 7 types according to the coupling of the matrices. For the sake of simplicity, isotropic chiral medium is mainly focused in this thesis.

In the past 20 years, chiral metamaterial was one of the famous research topics in matter physics. Metamaterials require the permittivity and permeability are both smaller than 0 such that the refractive index can be negative. In chiral materials, the

Table 1.2: Classification of chiral media. [26]

Coupling parameters	Classes
$\kappa \neq 0$, $\mathbf{N} = \mathbf{0}$, $\mathbf{J} = \mathbf{0}$	Isotropic chiral medium (Pasteur medium)
$\kappa \neq 0$, $\mathbf{N} \neq \mathbf{0}$, $\mathbf{J} = \mathbf{0}$	Anisotropic chiral medium
$\kappa = 0$, $\mathbf{N} \neq \mathbf{0}$, $\mathbf{J} = \mathbf{0}$	Pseudochiral medium
$\kappa = 0$, $\mathbf{N} = \mathbf{0}$, $\mathbf{J} \neq \mathbf{0}$	Omega medium
$\kappa \neq 0$, $\mathbf{N} = \mathbf{0}$, $\mathbf{J} \neq \mathbf{0}$	Chiral omega medium
$\kappa = 0$, $\mathbf{N} \neq \mathbf{0}$, $\mathbf{J} \neq \mathbf{0}$	Pseudochiral omega medium
$\kappa \neq 0$, $\mathbf{N} \neq \mathbf{0}$, $\mathbf{J} \neq \mathbf{0}$	General reciprocal bi-anisotropic medium

handedness of chirality results in different refractive indices in opposite directions. The refractive index of isotropic chiral materials can be written as [23, 29]

$$n_{\pm} = \sqrt{\varepsilon\mu} \pm \kappa. \tag{1.4}$$

Negative refractive index can be achieved without requiring ε and μ both smaller than 0. The studies on chiral metamaterials are still ongoing, whereas the objectives are different from the past. Most studies focus on using metamaterials to achieve particular physical phenomena rather than investigating its properties nowadays, for examples, original target of transformation optics — illusion effects [1–6] and non-trivial topological phase of chiral metamaterials [19, 21, 22]. Chiral metamaterials are commonly not included in the topic of transformation optics because coordinate transformation is not valid for transforming a simple anisotropic medium to a bi-anisotropic medium [8]. In the following sections and chapters, the ideas of the transforming simple anisotropic media to bi-anisotropic media are discussed, such that chiral metamaterials may be able to take into consideration.

1.3 Reviews on Transformation optics

1.3.1 Ideas of transformation optics

The main idea of transformation optics is based on the invariances of Maxwell's equations and Helmholz equation under coordinate transformation [1–8]. The Faraday's and Ampere's laws in macroscopic scale are

$$\boldsymbol{\nabla} \times \mathbf{E} + i\omega \mathbf{B} = \mathbf{0},\ \boldsymbol{\nabla} \times \mathbf{H} - i\omega \mathbf{D} = \mathbf{J_f}, \tag{1.5}$$

where free electrical current $\mathbf{J_f}$ is assumed to be $\mathbf{0}$. As mentioned in previous section, the macroscopic fields are following the constitutive relations corresponding to the types of materials. The constitutive relations of simple anisotropic materials are

$$\mathbf{D} = \varepsilon_0 \boldsymbol{\varepsilon} \mathbf{E},\ \mathbf{B} = \mu_0 \boldsymbol{\mu} \mathbf{H}, \tag{1.6}$$

In the coordinate space $\mathbf{x}$, Maxwell's equations in simple anisotropic materials are

$$\boldsymbol{\nabla} \times \mathbf{E}(\mathbf{x}) + i\omega \boldsymbol{\mu}(\mathbf{x}) \mathbf{H}(\mathbf{x}) = \mathbf{0},\ \boldsymbol{\nabla} \times \mathbf{H}(\mathbf{x}) - i\omega \boldsymbol{\varepsilon}(\mathbf{x}) \mathbf{E}(\mathbf{x}) = \mathbf{0}. \tag{1.7}$$

If there is a transformation from space $\mathbf{x}$ to $\mathbf{x}'$, where $\mathbf{x}' = \mathbf{x}'(\mathbf{x})$, the relations of the macroscopic EM fields between two spaces are

$$\mathbf{E}'(\mathbf{x}') = (\mathbf{A}^T)^{-1} \mathbf{E}(\mathbf{x}),\ \mathbf{H}'(\mathbf{x}') = (\mathbf{A}^T)^{-1} \mathbf{H}(\mathbf{x}), \tag{1.8}$$

where $\mathbf{A}$ is a Jacobian matrix with components $A_{ij} = \partial x_i' / \partial x_j$. The transformation is according to contravariant bases rather than covariant bases. The details can be

found in Appendix A.1. Due to the invariance of Maxwell's equations, equation (1.7) in the transformed space should be maintained but all symbols and operators are following with prime($'$) to emphasize the symbols are in the transformed space. i.e.,

$$\nabla' \times \mathbf{E}'(\mathbf{x}') + i\omega\boldsymbol{\mu}'(\mathbf{x}')\mathbf{H}'(\mathbf{x}') = \mathbf{0},\ \nabla' \times \mathbf{H}'(\mathbf{x}') - i\omega\boldsymbol{\varepsilon}'(\mathbf{x}')\mathbf{E}'(\mathbf{x}') = \mathbf{0}. \tag{1.9}$$

As shown in Fig. 1.1, the light beam in the transformed space still follows the original trajectory corresponding to its original coordinates [1–8]; in other words, the trajectory of the light beam can be controlled by adjusting the Jacobian matrix such that some "unrealistic" physical phenomena in conventional views can be easily achieved. The permittivity and permeability tensors in the transformed space are

$$\boldsymbol{\varepsilon}'(\mathbf{x}') = \frac{\mathbf{A}\boldsymbol{\varepsilon}(\mathbf{x})\mathbf{A}^T}{\det\mathbf{A}}, \quad \boldsymbol{\mu}'(\mathbf{x}') = \frac{\mathbf{A}\boldsymbol{\mu}(\mathbf{x})\mathbf{A}^T}{\det\mathbf{A}}, \tag{1.10}$$

which will be the physical parameters when the materials are constructed in reality. The mathematical foundations of transformation optics are shown in Appendix A.2. Such relations was simply regraded as a mathematical techniques to solve the wave equations before Pendry *et. al.* [1] and Leonhardt [2] proposed engineering the invisibility cloaks, super-scatters and super-absorbers by guiding the trajectory of light [3, 4]. This theory has become one of the famous theoretical designing tools now. The success in experimental demonstration of invisibility cloaks has also confirmed the validity of this theory [7].

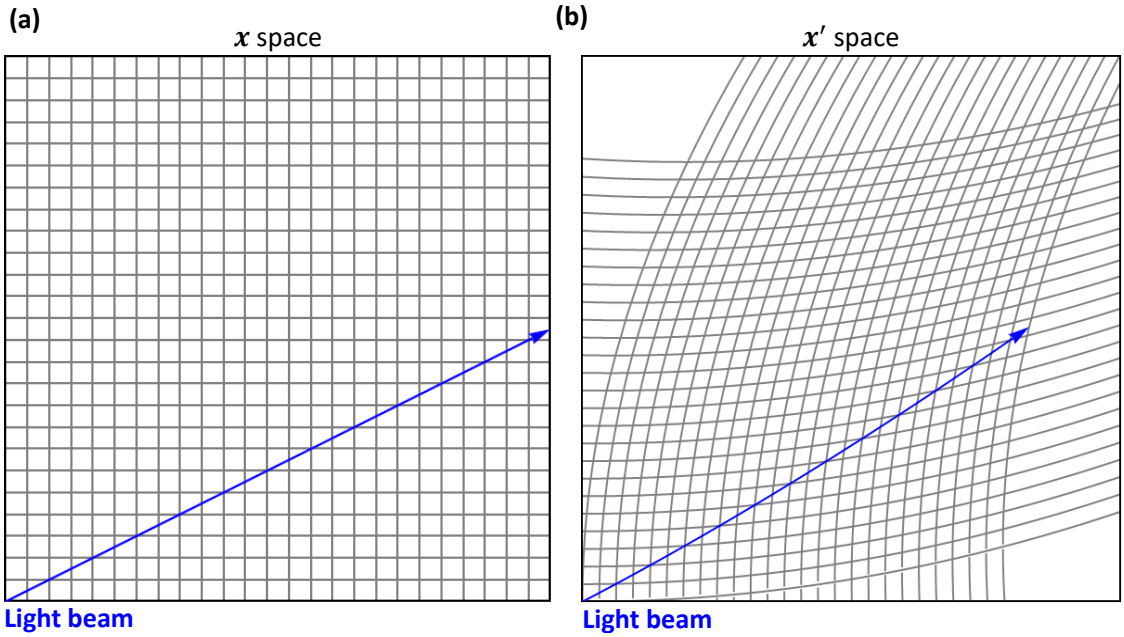

Figure 1.1: (a) The trajectory of the light beam in the original space. The original space is chosen to be vacuum due to simplicity. (b) The trajectory of the light beam in the transformed space. The path of the light beam is changed after coordinate transformation, but it still follows its original trajectory in the original space.

1.3.2 Transformation optics meets chirality

As mentioned before, the constitutive relations of bi-anisotropic and simple anisotropic materials are different due to the occurrence of optical activities in bi-anisotropic medium. Since non-reciprocity is not included in this study, the constitutive relations of chiral materials are

$$\mathbf{D} = \varepsilon_0 \boldsymbol{\varepsilon} \mathbf{E} - i\sqrt{\varepsilon_0 \mu_0}\, \boldsymbol{\kappa}^T \mathbf{H},\ \mathbf{B} = i\sqrt{\varepsilon_0 \mu_0}\, \boldsymbol{\kappa} \mathbf{E} + \mu_0 \boldsymbol{\mu} \mathbf{H}, \tag{1.11}$$

where $\boldsymbol{\kappa}(\mathbf{x})$ is the chirality tensor. Maxwell's equations (1.7) should be modified as:

$$\begin{aligned} \boldsymbol{\nabla} \times \mathbf{E}(\mathbf{x}) - \ \omega\sqrt{\varepsilon_0 \mu_0}\, \boldsymbol{\kappa}(\mathbf{x}) \mathbf{E}(\mathbf{x}) + i\omega \boldsymbol{\mu}(\mathbf{x}) \mathbf{H}(\mathbf{x}) = \mathbf{0}, \\ \boldsymbol{\nabla} \times \mathbf{H}(\mathbf{x}) - \ \omega\sqrt{\varepsilon_0 \mu_0}\, \boldsymbol{\kappa}^T(\mathbf{x}) \mathbf{H}(\mathbf{x}) - i\omega \boldsymbol{\varepsilon}(\mathbf{x}) \mathbf{E}(\mathbf{x}) = \mathbf{0}. \end{aligned} \tag{1.12}$$

Because it is expected that there is a conformal mapping between simple anisotropic medium and general reciprocal bi-anisotropic medium, Maxwell's equations (1.9) in the transformed space should be maintained. Clearly, Maxwell's equations in two spaces are no longer invariant, and thereby other transformation methods should be considered such that the transformation matrix can eliminate the chirality tensor. Thus, different from normal approaches of transformation optics, the transformation matrix is also an unknown in this situation. There is a remark that although **A** will still be used to represent the transformation matrix, it will no longer be a Jacobian matrix. i.e., $A_{ij} \neq \partial x'_i/\partial x_j$. After some mathematical calculations (see Appendix B), a contradiction appears during the transformation:

$$\epsilon^{ijk}[(\partial_j A^{\alpha}{}_{k})E'_{\alpha}] - \omega\sqrt{\varepsilon_0\mu_0}\kappa^{ij}A^{\alpha}{}_{j}E'_{\alpha} = 0 \tag{1.13}$$

and

$$\epsilon^{ijk}[(\partial_j A^{\alpha}{}_{k})H'_{\alpha}] - \omega\sqrt{\varepsilon_0\mu_0}\kappa^{ji}A^{\alpha}{}_{j}H'_{\alpha} = 0, \tag{1.14}$$

where α and i, j, k are $1, 2, 3$, and ϵ_{ijk} is the Levi-Civita symbol. Here, Einstein notation is implied. In order to resolve this contradiction, different transformation matrices of **E** and **H** fields should be applied. In general, this idea is valid for 3-dimensional structures; however, for the sake of simplicity, only isotropic chirality ($\kappa^{ij} = \kappa\delta^{ij}$) and 1D systems are considered in this study. The transformation matrix can be independent of the fields by choosing suitable parameters; hence, the transformations of the fields and tensors, equations (1.8) and (1.10), can be maintained. The mathematical details of transformation from simple anisotropic medium to general reciprocal bi-anisotropic medium are shown in Appendix B. Also, it is trivial

that the transformation matrix is dependent on frequency because optical activities are frequency-dependent phenomena in general. For instance, optical rotatory dispersion is owing to different rotation angles of different colours of visible light [30]. If transformations of **E** and **H** between two spaces are achieved, the theories of simple anisotropic materials can be totally applied in chiral materials; furthermore, chiral materials which are new, complicated and having an analytical wave solution can be easily designed when simple anisotropic materials which have an analytical wave solution are considered as reference structures.

1.4 Reviews on topological theories in 1D phononic system

1.4.1 Zak phase

In 1983, Berry [31] realized a geometric phase in quantum mechanics which can give observable effects. One of the famous examples is Aharonov-Bohm effect [32]. In 1989, Zak [33] had picked up the theory of Berry' s phase and applied it in 1D electronic periodic systems. Because of the similarity of Schrödinger's equation and Maxwell's equations, Hadlane and Raghu [11] had successfully transferred the topological theories from electronic systems to photonic crystals in 2005 [14], and this idea had been confirmed by experimental results in 2008 [12]. A new phases of matter called topological insulators is discovered from this theory. Photonic topological insulator can transmit EM waves without back-reflection [14]. Thus, this theory—topological photonics had been rapidly developed and become a popular realm in photonics. In this section, the topological theories related to my study are

going to be reviewed.

The Zak phase of the nth isolated band can be numerically calculated by

$$\Phi_n^{\text{Zak}} = i \sum_m \ln\langle\Psi_m|\Psi_{m+1}\rangle + i \ln\langle\Psi_f|\Psi_i\rangle, \tag{1.15}$$

where $|\Psi_m\rangle$ is the normalized eigenstate at the mth Bloch wave vector $\mathbf{k}_m$; $|\Psi_i\rangle$ and $|\Psi_f\rangle$ are the initial and final eigenstates of the nth isolated band such that the path in $\mathbf{k}$ space is a close loop. In general, the Zak phase of an isolated band can be an arbitrary complex number [34]. It can be quantized if certained symmetries existed in the system and the point of the symmetry is picked up. An isotropic binary photonic crystal is taken as an example. The edge of a white slab is chosen as an origin in Fig. 1.2(a), whereas the center of a white slab, the inversion center, is chosen as an origin in Fig. 1.2(c). Figs. 1.2(b) and (d) show that the band structures are not affected by the positions of the origin; however, Zak phases do depend on it since the eigenvectors will be changed by the choices of origin. In this example, the eigenvectors of the system shown in Fig 1.2(a) are complex values; in contrast, the eigenvectors of the system Fig. 1.2(c) are real, and thereby the Zak phases can be quantized to 0 or π.

Zak phase is a topological invariance, which is unchanged when the system undergoes continuous deformation. The reason will be briefly explained here. According to the transformation law, the relation of the numerical eigenvectors between two position spaces is

$$|\Psi'_m(\mathbf{x}')\rangle = A(\mathbf{x})|\Psi_m(\mathbf{x})\rangle, \tag{1.16}$$

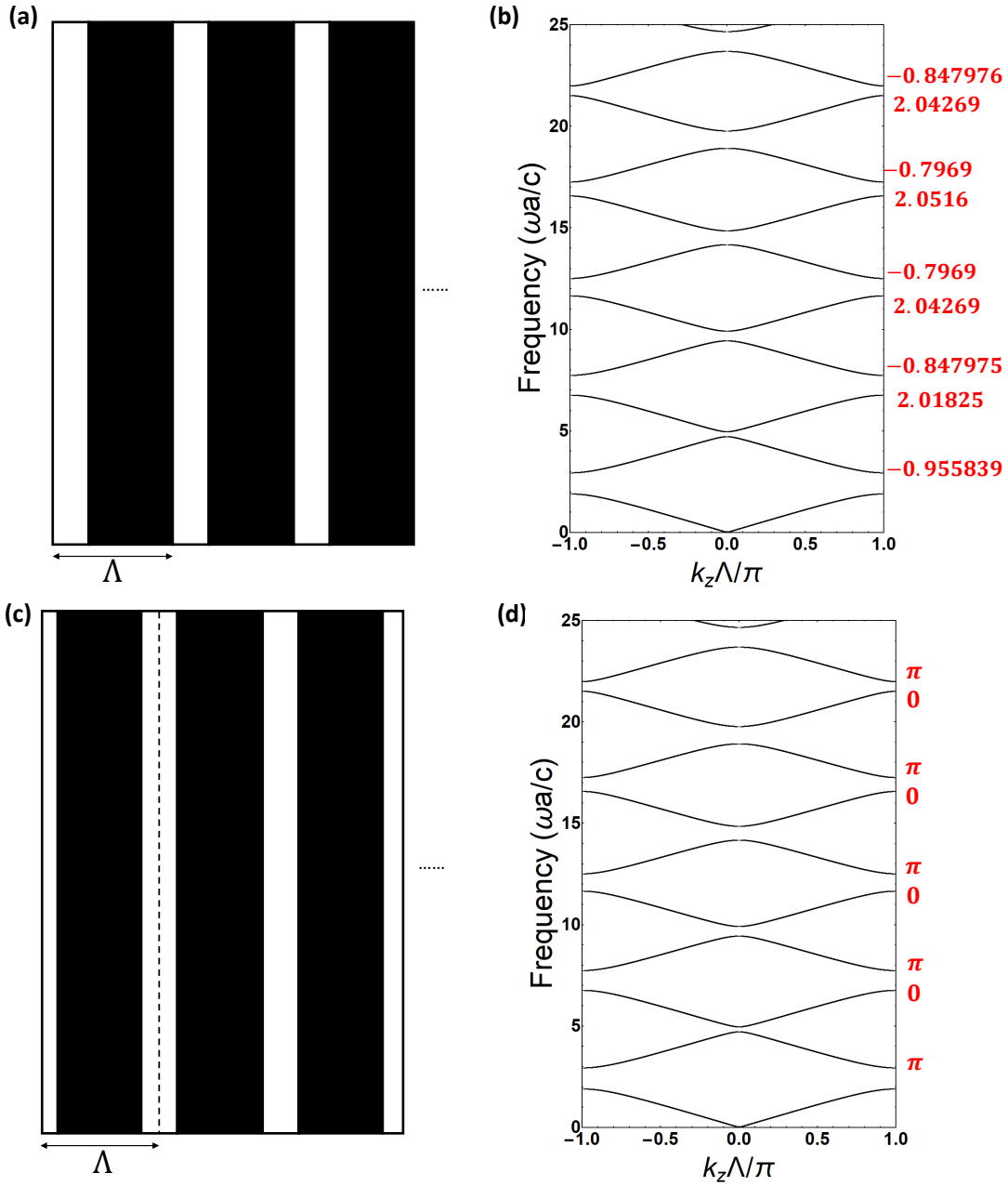

Figure 1.2: (a) and (c) are the structures of the photonic crystals. Double-headed arrows mark the chosen unit cells, and Λ is the width of a unit cell. The dielectric and magnetic parameters of the white slab are given by $\varepsilon = 4$ and $\mu = 1$, and the width is 0.3Λ. The black slab is vacuum slab and the width is 0.7Λ. (b) and (d) are the band structures of the photonic crystals shown in (a) and (c) respectively. The Zak phase of each isolated band is labelled. The Zak phases can be quantized when the center of white (or black) slab is chosen as the origin, the structure shown in (c). The Zak phase of the lowest band cannot be determined by equation (1.15) due to existence of degenerated point at $\omega = 0$.

where A is a transformation operator. Because $|\Psi'_m(\mathbf{x}')\rangle$ and $|\Psi_m(\mathbf{x})\rangle$ are normalized bases and $A(\mathbf{x})$ is assumed to be real, the inverse of $A(\mathbf{x})$ is equal to its transpose. Thus,

$$\ln\langle\Psi'_m|\Psi'_{m+1}\rangle = \ln\langle\Psi_m|\Psi_{m+1}\rangle. \tag{1.17}$$

In principle, according to equation (1.13) or (1.14), the transformation matrix for eliminating the chirality parameter should be dependent on frequency and thereby $\langle\Psi_m|A_m^\dagger\nabla_{\mathbf{k}}A_m|\Psi_m\rangle\delta\mathbf{k}$ should be added in equation (1.17). In practice, the period of the transformed structure cannot be determined if the transformation is frequency-dependent. Mathematically speaking, we first suppose the transformation operators at frequencies ω_1 and ω_2 are $A(\mathbf{x},\omega_1)$ and $A(\mathbf{x},\omega_2)$ respectively. Despite of $A(\mathbf{x}+\mathbf{a_1},\omega_1) = A(\mathbf{x},\omega_1)$ and $A(\mathbf{x}+\mathbf{a_2},\omega_2) = A(\mathbf{x},\omega_2)$, it cannot be ensured $\mathbf{a_1} = \mathbf{a_2}$. Therefore, adjustments to the chirality parameter are needed when the designed chiral material acts as a unit cell of a photonic crystal. Examples will be shown in chapter 2.

1.4.2 Existence of topological edge states in 1D photonic crystals

Interface states can exist between two connected photonic crystals. If the interface states can be predicted by some topological invariances, it is possible to say the interface states are topological protected by certain symmetries. The interface states of a system composed of two 1D isotropoic binary photonic crystals can be

predicted by the sign of the surface impedance in the photonic band gap [35, 36]:

$$\mathrm{sgn}\left[\zeta^{(n)}\right] = (-1)^{n+l}\,\exp\left(i\sum_{p=0}^{n-1}\Phi_p^{\mathrm{Zak}}\right), \tag{1.18}$$

where the integer l is the number of degenerated points below the nth photonic band gap. Interface state appears if $\mathrm{sgn}\left[\zeta^{(n)}\right]$ of two connected photonic crystals is opposite in a common gap. Due to existence of a degenerated point at the lowest frequency ($\omega = 0$), the Zak phase of the lowest band (0th band) is determined by [35, 36]

$$\exp\left(\Phi_0^{\mathrm{Zak}}\right) = \mathrm{sgn}\left[1 - \frac{\varepsilon_A\mu_B}{\varepsilon_B\mu_A}\right]. \tag{1.19}$$

To ensure the Zak phase of each band can be quantized to 0 or π, a point of symmetries should be taken as an origin of the system. By supposing the propagation direction of light along z-axis, this type of binary photonic crystals obeys z-inversion symmetry and the inversion centers are at the center of each slab [35]. For clear explanation, the first and second slabs are named as A and B slabs respectively. "a half of slab A - slab B - a half of slab A" is chosen as the composition of a unit cell of a photonic crystal, which is the same structure shown in Fig. 1.2(c). To guarantee the mid-gap positions of two binary photonic crystals are the same, optical path lengths $n_A d_A + n_B d_B$ of the photonc crystals should be kept [35, 36] as the same, where n and d are the refractive index and the width of a slab respectively; also, the width of a unit cell is $\Lambda = d_A + d_B$. The transmission spectrum of a system composed of 10 unit cells of two 1D isotropic binary photonic crystals is shown in Fig. 1.3(a), and the band structures of photonic crystals 1 and 2 are respectively shown in Figs. 1.3(b) and (c). The parameters of photonic crystal 1 are given by

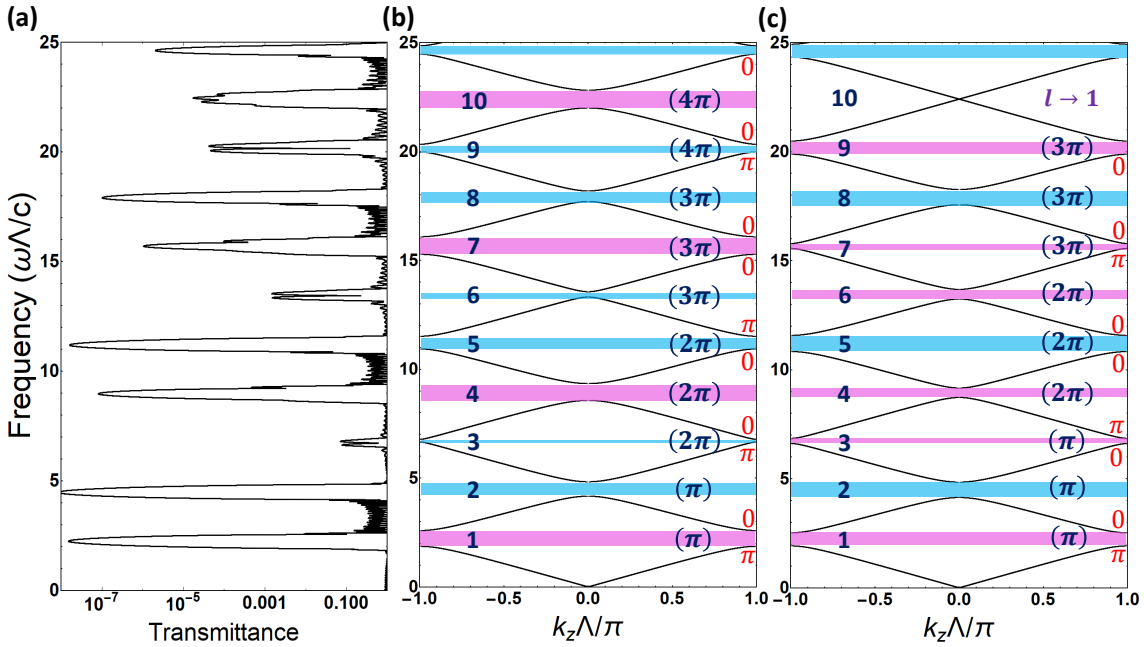

Figure 1.3: (a) The transmission spectrum of a system composed of 10 unit cells of isotropic binary photonic crystal 1 on the left side and 10 unit cells of isotropic binary photonic crystal 2 on the right side. The parameters of photonic crystal 1 are given by $\varepsilon_A = 3.2$, $\varepsilon_B = \mu_A = \mu_B = 1$, $d_A = 0.51\Lambda$ and $d_B = 0.49\Lambda$, and the parameters of photonic crystal 2 are given by $\varepsilon_A = 2.868$, $\varepsilon_B = \mu_A = \mu_B = 1$, $d_A = 0.58\Lambda$ and $d_B = 0.42\Lambda$. (b) and (c) are the band structures of photonic crystal 1 and 2 respectively. In both band structures, the Zak phase of each band are denoted near the band and the number in the brackets are the sum of the Zak phases below the gaps; also, the magenta and cyan strips represent the gaps with $\zeta > 0$ and $\zeta < 0$ respectively.

$\varepsilon_A = 3.2$, $\varepsilon_B = \mu_A = \mu_B = 1$, $d_A = 0.51\Lambda$ and $d_B = 0.49\Lambda$. The parameters of photonic crystal 2 are given by $\varepsilon_A = 2.868$, $\varepsilon_B = \mu_A = \mu_B = 1$, $d_A = 0.58\Lambda$ and $d_B = 0.42\Lambda$. The interface states appear in the 3rd, 6th and 9th gaps, in which ζ of the photonic crystals are opposite signs. This theory can also be generalized to 1D isotropic multilayered structures [37]. If a material is designed via transformation optics, it is usually anisotropic and inhomogenuous; thus, equation (1.18) may not be directly applied. Specific parameters will be chosen and "second transformation" will be considered so that equation (1.18) is still suitable to predicting the interface states.

1.5 Conclusions

In this chapter, the concepts of chiral materials, general ideas of transformation optics and topological theories of 1D photonic crystals are briefly reviewed. Due to occurrence of natural optical activities in chiral materials, the parity inversion symmetry is broken, and **D** and **B** fields depend on both **E** and **H** fields. Thus, a wider parameter space can be provided for the realization of different topological phases. The applications of chiral materials have been briefly introduced also. On the other hand, the ideas of transformation optics have been illustrated. Transformation optics is a mathematical technique based on coordinate transformation. The paths of light can be controlled by the Jacobian matrix so that some "unrealistic" phenomena in conventional view can be easily achieved. Although most studies focus on the transformation between simple anisotropic materials, a conformal mapping between simple anisotropic materials and chiral materials can also be achieved. Because of invariance of Maxwell's equations under coordinate transformation, other transformation methods should be considered so that the chirality tensor can be eliminated during the space transformation. Instead of the trajectory, optical activity can be controlled by the flexibility of the transformation matrix. The general idea of the transformation is introduced. Finally, the concepts of topology in 1D photonic systems are reviewed. Zak phase is one of the topological invariances in 1D photonic systems, which can be retained after continuous spatial deformation. If a system contains certain symmetries and a point of the symmetries is picked up, the Zak phase of each isolated band can be quantized to 0 or π. The existence of interface states of a system composed of two 1D isotropic binary photonic crystals can be predicted by the signs of surface impedance in the nth gap, $\mathrm{sgn}[\zeta^{(n)}]$. Interface

states must exist if ζ of the photonic crystals in common gaps are opposite signs.

Chapter 2

Transformation optics and chiral photonic crystals

The theory of transformation optics is based on the invariance of Maxwell's equations under coordinate transformation [1–6]. Despite of spatial transformation, the light beam still follows the original trajectory corresponding to its original coordinates; in order words, the paths of light in the transformed space can be controlled by Jocobian matrix. Thus, such "unrealistic" effects in conventional views as invisibility cloaks can be easily achieved. In this study, a conformal mapping between 1D isotropic chiral medium and 1D simple medium is mainly considered. Because of the differences in the constitutive relations, other transformation methods should be considered instead of coordinate transformation such that a gauge field can be raising for eliminating the chirality tensor. In this chapter, the details of transformation between 1D simple anisortropic medium and 1D anisotropic medium with isotropic chirality are discussed. Instead of the trajectory, optical rotation can be

controlled by the transformation matrix. Then, by choosing different parameters, the dispersion relations of the 1D chiral photonic crystals composed of the designed chiral materials are examined.

2.1 Transformation from isotropic chiral medium to simple medium

To ensure the chirality parameter can be erased, a transformation from anisotropic medium with isotropic chirality to simple anisotropic medium is considered. Because the chiral materials are expected to construct in reality, the chiral medium is named to be "physical space" (x, y, z) and the simple medium is named to be "virtual space" (x', y', z'). In order words, the transformation from the physical space (x, y, z) to the virtual space (x', y', z') is first considered for finding out the transformation matrix; then, the wave properties in the physical space will be predicted by the properties in the virtual space. Electromagnetic waves are governed by Maxwell's equations and the constitutive relations of the medium. By supposing the EM waves are propagating along z-axis and the time component is harmonic, the transverse components of the fields in 1D system can be written as $\mathbf{F}(\omega, z)\exp(-i\omega t) = \big(E_x(\omega, z)\, E_y(\omega, z)\, Z_0 H_x(\omega, z)\, Z_0 H_y(\omega, z)\big)^T \exp(-i\omega t)$, where Z_0 is the impedance in vacuum and ω is the angular frequency of the EM waves. After combining with the constitutive relations of isotropic chiral medium, Faraday's and Ampere's laws can be expressed as

$$\frac{d}{dz}\mathbf{F}(\omega, z) = \frac{i\omega}{c}\Big[\mathbf{M}(\omega, z) + i\mathbf{K}(\omega, z) + \mathbf{L}(\omega, z)\Big]\mathbf{F}(\omega, z), \tag{2.1}$$

where the 4×4 matrices are

$$\mathbf{M}(\omega, z) = \begin{pmatrix} 0 & 0 & \mu_{21} & \mu_{22} \\ 0 & 0 & -\mu_{11} & -\mu_{12} \\ -\varepsilon_{21} & -\varepsilon_{22} & 0 & 0 \\ \varepsilon_{11} & \varepsilon_{12} & 0 & 0 \end{pmatrix} \tag{2.2}$$

,

$$\mathbf{K}(\omega, z) = \kappa \begin{pmatrix} 0 & 1 & 0 & 0 \\ -1 & 0 & 0 & 0 \\ 0 & 0 & 0 & 1 \\ 0 & 0 & -1 & 0 \end{pmatrix} \tag{2.3}$$

and

$$\begin{aligned} \mathbf{L}(\omega, z) =& \frac{1}{\varepsilon_{33}\mu_{33} - \kappa^2} \begin{pmatrix} 0 & 0 & -\mu_{23}\mu_{31}\varepsilon_{33} & -\mu_{23}\mu_{32}\varepsilon_{33} \\ 0 & 0 & \mu_{13}\mu_{31}\varepsilon_{33} & \mu_{13}\mu_{32}\varepsilon_{33} \\ \varepsilon_{23}\varepsilon_{31}\mu_{33} & \varepsilon_{23}\varepsilon_{32}\mu_{33} & 0 & 0 \\ -\varepsilon_{13}\varepsilon_{31}\mu_{33} & -\varepsilon_{13}\varepsilon_{32}\mu_{33} & 0 & 0 \end{pmatrix} \\ &+ \frac{i\kappa}{\varepsilon_{33}\mu_{33} - \kappa^2} \begin{pmatrix} -\varepsilon_{31}\mu_{23} & -\varepsilon_{32}\mu_{23} & 0 & 0 \\ \varepsilon_{31}\mu_{13} & \varepsilon_{32}\mu_{13} & 0 & 0 \\ 0 & 0 & \varepsilon_{23}\mu_{31} & \varepsilon_{23}\mu_{32} \\ 0 & 0 & -\varepsilon_{13}\mu_{31} & -\varepsilon_{13}\mu_{32} \end{pmatrix}. \end{aligned} \tag{2.4}$$

ε_{ij} and μ_{ij} represent the elements of relative dielectric permittivity and magnetic permeability tensors, which are dispersive and inhomogeneous along z-axis in general. c is the speed of light in vacuum. The differential matrix equation in the

virtual space can be easily found by substituting $\kappa = 0$ into equation (2.1) and add prime($'$) to all symbols. i.e.,

$$\frac{d}{dz'}\mathbf{F}'(\omega, z') = \frac{i\omega}{c}\Big[\mathbf{M}'(\omega, z') + \mathbf{L}'(\omega, z')\Big]\mathbf{F}'(\omega, z'). \tag{2.5}$$

Since a conformal mapping between the physical and virtual spaces is expected, the relation of the wave solutions in two spaces should be $\mathbf{F}'(\omega, z') = \mathbf{R}(\omega, z)\,\mathbf{F}(\omega, z)$, where $\mathbf{R}(\omega, z)$ is a transformation matrix. As mentioned in chapter 1, it is trivial that the transformation matrix is dependent on frequency because optical activities are frequency-dependent phenomena. Consequently, the fields with different frequencies are belongs to different virtual spaces. In general, the transformation is extremely complicated if $\mathbf{L}$ is included, whereas the case of $\mu_{31} = \mu_{32} = \mu_{13} = \mu_{23} = 0$ and $\varepsilon_{31} = \varepsilon_{32} = \varepsilon_{13} = \varepsilon_{23} = 0$ is chosen here for reducing the complexity. Hence, a simpler transformation can be obtained because of $E_z = H_z = 0$ and $\mathbf{L} = \mathbf{0}$. According to equation (1.8), the transformation matrix $\mathbf{R}(\omega, z)$ is equal to $\mathbf{I}_{2\times 2} \otimes [[(\mathbf{A}^T)^{-1}]_{ab}]$, where $\mathbf{I}$ is an identity matrix and $a, b = 1, 2$. The differential matrix in the transformed space becomes:

$$\begin{aligned}\frac{d}{dz'}\mathbf{F}'(z') = \frac{1}{A_{33}}\Big[&\frac{i\omega}{c}\mathbf{R}(z)\mathbf{M}(z)\mathbf{R}^{-1}(z) \\ &- \Big(\frac{\omega}{c}\mathbf{R}(z)\mathbf{K}(z)\mathbf{R}^{-1}(z) + \mathbf{R}(z)\Big[\frac{d}{dz}\mathbf{R}^{-1}(z)\Big]\Big)\Big]\mathbf{F}'(z'),\end{aligned} \tag{2.6}$$

where $A_{33} = 1$ is chosen due to its arbitrariness. The expressions of ω in the matrices are omitted in this step. The transformation is supposed to eliminate the chirality parameter, so the second term in the square bracket should be vanished. A famous

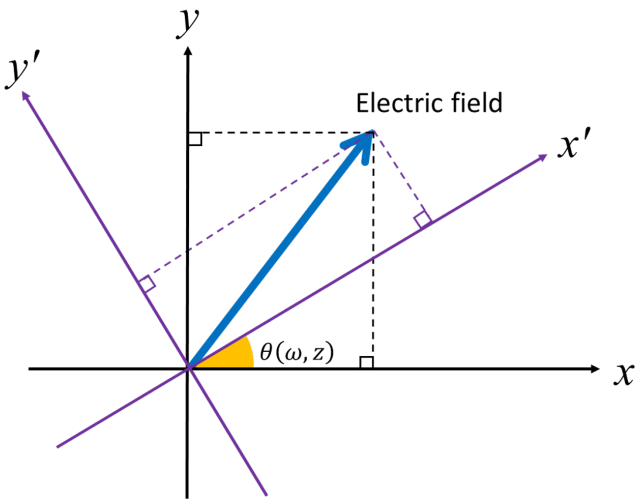

Figure 2.1: $\mathbf{x}$ and $\mathbf{x}'$ spaces at particular z. The virtual space is rotating the x-y planes along z-axis in the physical space.

transformation called Oseen transformation [38] can be obtained:

$$\begin{aligned}\mathbf{R}(\omega, z) &= \mathbf{I}_{2\times 2} \otimes [R_{ab}] \\ &= \mathbf{I}_{2\times 2} \otimes \begin{pmatrix} \cos\theta & \sin\theta \\ -\sin\theta & \cos\theta \end{pmatrix},\end{aligned} \tag{2.7}$$

where

$$\theta(\omega, z) = \frac{\omega}{c} \int_{z_0}^{z} \kappa(\omega, u)\, du \tag{2.8}$$

and $R_{ab} = [(\mathbf{A}^T)^{-1}]_{ab}$ $(a, b = 1, 2)$. The transformation is a rotation of rotating the x-y planes along z-axis, and the angle of rotation is dependent on frequency in general. A schematic diagram of the transformation is shown in Fig. 2.1. This result agrees with the phenomena occurred in isotropic chiral materials, optical rotation and optical rotatory dispersion. The angle of optical rotation at particular frequency can be controlled by the transformation matrix. I should emphasize that Oseen transformation is not the only transformation. If $\mathbf{L} \neq \mathbf{0}$, the transformation will become more complicated. More details can be found in Appendix C. Second,

$\theta(z)$ still follows reciprocity. Because a minus sign should be inserted when the incident light propagates from the opposite direction, the directions of rotation is reversed if the position of the observer is assumed to be unchanged.

After the transformation, finding the wave solution in the virtual space becomes a matter of course. Although the differential equation (2.5) can be solved by numerical integration, it will be more attractive if the system has an analytically solvable wave solution in the virtual space. This idea is the same as the normal approach of transformation optics. Vacuum are usually considered as a reference space so that EM waves in the transformed space can be easily guided. The dielectric permittivity and magnetic permeability tensors in the virtual space (achiral medium) are assumed to be homogeneous and non-dispersive so that EM waves in the virtual space are just plane waves. The wave solution in the virtual space is

$$\mathbf{F}'(\omega, z) = \exp\Big[\frac{i\omega\Delta z}{c}\mathbf{M}'\Big]\mathbf{F}'(\omega, z_0), \tag{2.9}$$

where $\Delta z = z - z_0$ and $\mathbf{M}'$ is now a constant matrix. The wave solution in the physical space (isotropic chiral medium) is

$$\begin{aligned}\mathbf{F}(\omega, z) &= \mathbf{R}^{-1}(\omega, z)\ \mathbf{F}'(\omega, z) \\ &= \mathbf{R}^{-1}(\omega, z)\ \exp\Big[\frac{i\omega\Delta z}{c}\mathbf{M}'\Big]\mathbf{F}(\omega, z_0).\end{aligned} \tag{2.10}$$

Note that $\mathbf{R}(\omega, z_0)$ is a 4×4 identity matrix. In Figs. 2.2 (a) and (b), the schematic diagrams of the electric fields in the physical and virtual spaces are shown respectively. In the physical space, the field is rotating along z-axis, but it is just a plane wave in the virtual space. For convenience, the permittivity and permeabil-

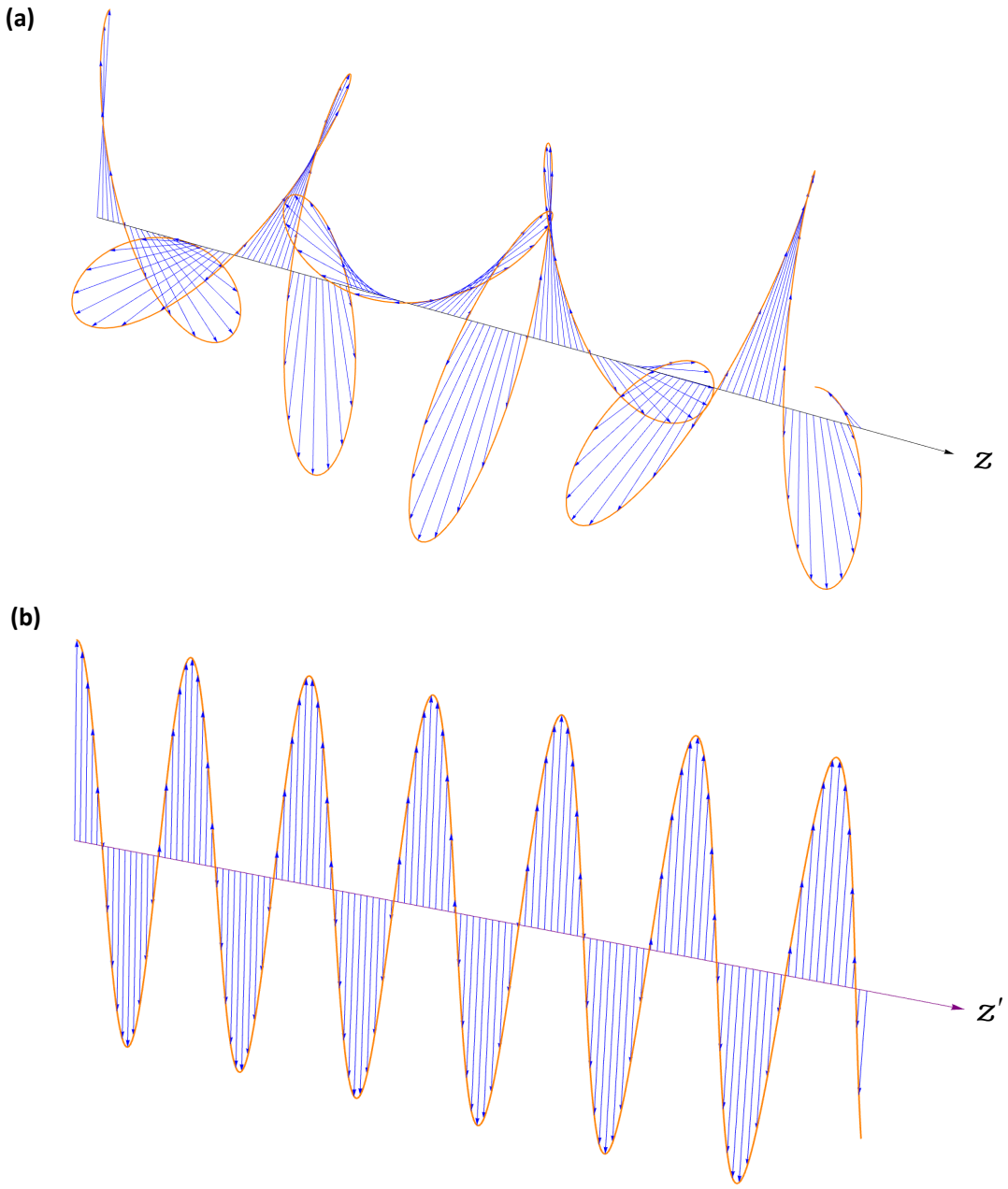

Figure 2.2: (a) Electric field propagating in an isotropic chiral medium (physical space) at a particular time. The electric field is rotating along z-axis. (b) Electric field propagating in a transformed simple medium (virtual space) at a particular time. The electric field becomes a plane wave.

ity tensors in the virtual space are further supposed to be $\mathrm{diag}(\varepsilon'_{11}, \varepsilon'_{22}, \varepsilon'_{33})$ and $\mathrm{diag}(\mu'_{11}, \mu'_{22}, \mu'_{33})$ respectively. The transformation laws of the tensors still follow equation (1.10). The permittivity tensor in the physical space can be found by

$$\begin{aligned} \boldsymbol{\varepsilon}' &= \frac{1}{\det\mathbf{A}}\,\mathbf{A}\boldsymbol{\varepsilon}(z)\mathbf{A}^T \\ \Rightarrow\quad \boldsymbol{\varepsilon}(z) &= \begin{pmatrix} \frac{\varepsilon'_{11}+\varepsilon'_{22}}{2} + \frac{\varepsilon'_{11}-\varepsilon'_{22}}{2}\cos 2\theta & \frac{\varepsilon'_{11}-\varepsilon'_{22}}{2}\sin 2\theta & 0 \\ \frac{\varepsilon'_{11}-\varepsilon'_{22}}{2}\sin 2\theta & \frac{\varepsilon'_{11}+\varepsilon'_{22}}{2} - \frac{\varepsilon'_{11}-\varepsilon'_{22}}{2}\cos 2\theta & 0 \\ 0 & 0 & \varepsilon'_{33} \end{pmatrix}. \end{aligned} \tag{2.11}$$

The permeability tensor can be found by simply replacing ε'_{ij} to μ'_{ij}. It should be careful that the permittivity and permeability tensors include unphysical functions, $\cos 2\theta$ and $\sin 2\theta$, where θ is a function of z and ω. Again, the reason of appearing these unphysical functions is that optical activities are frequency-dependent phenomena in general. This also leads to the period cannot be well-defined when the material acts as a unit cell of a photonic crystal. For instance, despite of $\boldsymbol{\varepsilon}(z + a_1, \omega_1) = \boldsymbol{\varepsilon}(z, \omega_1)$ and $\boldsymbol{\varepsilon}(z + a_2, \omega_2) = \boldsymbol{\varepsilon}(z, \omega_2)$, it cannot be ensured $a_1 = a_2$, so do $\boldsymbol{\mu}$ and κ. There are two methods for resolving this problem. First, the frequency of the incident light is fixed during the transformation (say ω_1), so that the transformation matrix $\mathbf{R}$ only depends on position z. As a result, there is an analytical wave solution to the designed chiral material only when the frequency of the incident light equals ω_1. The idea is also similar to normal approaches of transformation optics. The designed materials via transformation optics usually have a condition $\varepsilon = \mu$, which is usually valid at a particular frequency only. Second, an adjustment to the chirality parameter is made so that the transformation and the analytical solutions are valid for a wider frequency range. Second idea is taken

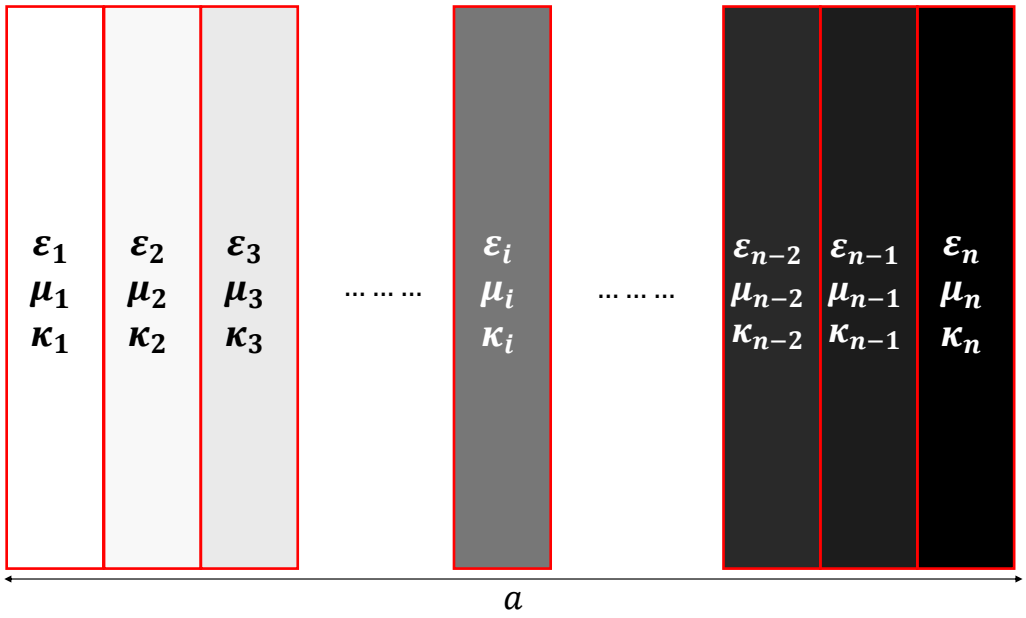

Figure 2.3: A schematic diagram of layer-by-layer method. The designed chiral material contains n layers and the width of the chiral material is a. Continuous functions $\boldsymbol{\varepsilon}$, $\boldsymbol{\mu}$ and $\boldsymbol{\kappa}$ can be obtained by connecting multiple layers. Each layer has different $\boldsymbol{\varepsilon}$, $\boldsymbol{\mu}$ and $\boldsymbol{\kappa}$.

into consideration in the following sections and chapters. There is a remark that the major objective of the methods is to make the structure angle θ independent of frequency, i.e., $\theta(\omega, z) \to \theta(z)$.

The designed chiral material can be fabricated in reality via layer-by-layer method. We can consider the chiral material is constructed by multiple layers, and each layer has different $\boldsymbol{\varepsilon}$, $\boldsymbol{\mu}$ and $\boldsymbol{\kappa}$. Mathematically speaking, by supposing the designed chiral material contains n layers and the width of the chiral material is a, the permittivity tensor of the ith layer is $\boldsymbol{\varepsilon}(z_i)$, where $z_i = z_0 + ia/n$. A schematic diagram is shown in Fig 2.3.

2.2 1D chiral photonic crystals

The techniques of transformation optics were used to design a chiral material. Instead of the trajectory, the angle of rotation can be controlled by the transformation matrix. A chiral photonic crystal can be constructed by repeating the designed material; however, as mentioned in previous section, the permittivity and permeability tensor in the physical space consist of unphysical functions. In order the result can be appropriate for a wider frequency range, the chirality parameter is reasonably chosen as $\kappa(\omega, z) \to \kappa_0(z)/\omega$ so that $\theta(\omega, z) \to \theta(z)$. There is a remark that the value of κ_0 should be large ($\sim 10^7$). Furthermore, $\theta(z)$ will not necessarily be a continuous function through whole space when the designed material acts as a unit cell of a photonic crystal. Modifications of the wave solution (2.10) and $\theta(z)$ are expected. In this section, by choosing suitable parameters, the dispersion relations of the chiral photonic crystals are examined.

Due to discontinuity of the electromagnetic tensors, the wave solution of the chiral photonic crystal composed of the designed chiral materials can be found by transfer-matrix method:

$$\mathbf{F}(\omega, z) = \mathbf{R}^{-1}(z - Na) \exp\Big[\frac{i\omega(z - Na)}{c}\mathbf{M}'\Big] \Big[\mathbf{R}^{-1}(a) \exp\Big[\frac{i\omega a}{c}\mathbf{M}'\Big]\Big]^N \mathbf{F}(\omega, 0), \tag{2.12}$$

where a is the width of a unit cell and N is a number of unit cells that the light passed through. i.e., $N = \lfloor z/a \rfloor$. $z_0 = 0$ is chosen as an origin of the photonic crystal. The dispersion relation of the chiral photonic crystals can be found by

Bloch's theorem:

$$\mathbf{R}^{-1}(a)\exp\Big(\frac{i\omega a}{c}\mathbf{M}'\Big)\mathbf{F}(\omega,0)=e^{ik_z a}\mathbf{F}(\omega,0), \tag{2.13}$$

where k_z is the Bloch wave vector. If the permittivity and permeability parameters in the virtual space are fixed, the dispersion relation will be dependent on the angle $\theta(a)$ (mod 2π) only. No matter what functions $\theta(z)$ they are, the band structures will still be the same if $\theta(a)$ (mod 2π) are the same. On the basis of this lemma, $\kappa_0(z)$ can be considered as a constant so that $\theta(z)$ becomes a linear function in a unit cell. For $z>0$, the structural "twisted" angle of the chiral photonic crystal can be expressed as

$$\theta(z)=\begin{cases}\theta_{max}\Big(\dfrac{z}{a}-\Big\lfloor\dfrac{z}{a}\Big\rfloor\Big) & ,\lfloor z/a\rfloor\in\mathbb{N}\\ \theta_{max} & ,\lfloor z/a\rfloor\notin\mathbb{N}\end{cases} \tag{2.14}$$

where $\theta_{max}=\theta(a)$ and $\theta(0)=0$. Floor function is included because θ is reset to initial value after a unit cell. i.e., $\theta(z+a)=\theta(z)$. There is a remark that $\theta(z)$ is directional, which means a minus sign should be added when the incident light propagates from opposite direction. The photonic band structures of $\theta(a)=0$, 0.25π, 0.5π, 0.75π, π and 1.25π are shown in Fig. 2.4. The permittivity and permeability tensors in the virtual space are given by $\mathrm{diag}(4,1,\varepsilon'_{33})$ and identity respectively, where ε'_{33} can be arbitrary because of $\mathbf{L}(z)=\mathbf{0}$. When $\theta(a)=0$, the structure is simple anisotropic and homogeneous, so there is no difference from the band structure in the virtual space. When $\theta(a)$ increases, the bands are splitting and photonic band gaps appear. The bands are splitting can be attributed to the

existence of chirality [28, 39], while the appearance of band gaps is due to the discontinuity of the dielectric permittivity tensors. At the lowest frequency, k_z is not equal to 0 may be due to the validity of the chosen chiral model at low frequency. According to one-resonance Condon model, the chirality parameter with single resonant frequency can be expressed as [9]

$$\kappa(\omega, z) = \frac{\omega}{\omega^2 - {\omega_0}^2} \kappa_0(z), \tag{2.15}$$

where ω_0 is the resonant frequency of chiraliy. In my chosen chiral model, $\omega \gg \omega_0$ has been considered so that $\kappa \propto 1/\omega$. When $\theta(a)$ increases to 0.5π, there appears the largest number of complete photonic band gaps. When $\theta(a)$ further increases, the gaps are closing and the bands are further splitting. When $\theta(a) = \pi$, the photonic band gaps are completely closed and the band structure is shifted to left (or right) by 1 compared to Fig. 2.4(a). When $\theta(a)$ further increases, the band structure starts returning back to the band structure of $\theta(a) = 0$. There are some properties of the band structures which can be further illustrated. The band structures of $\theta(a)$ and $\pi + \theta(a)$ can be overlapped by shifting either one of them to the left (or right) by 1, and the eigenvectors also follow the shifting, for example, Figs. 2.4(b) and (f). It should be careful that the similar results is also shown in the regions of $\theta(a) \in [0, 0.5\pi)$ and $(0.5\pi, \pi]$, for example, Figs. 2.4(b) and (d). Nevertheless, although the band structures found in $\theta(a) \in (0.5\pi, \pi]$ can overlap with the band structure of $\pi - \theta(a)$ by shifting either one of them to the left (or right) by 1, the eigenvectors are not following the shifting. Due to these reasons, it is adequate that only $\theta(a) \in [0, \pi]$ is considered. The Mathematical details can be found in Appendix D. $\theta(a) = \pi/2$ will be mainly focused in the following chapters because there appears

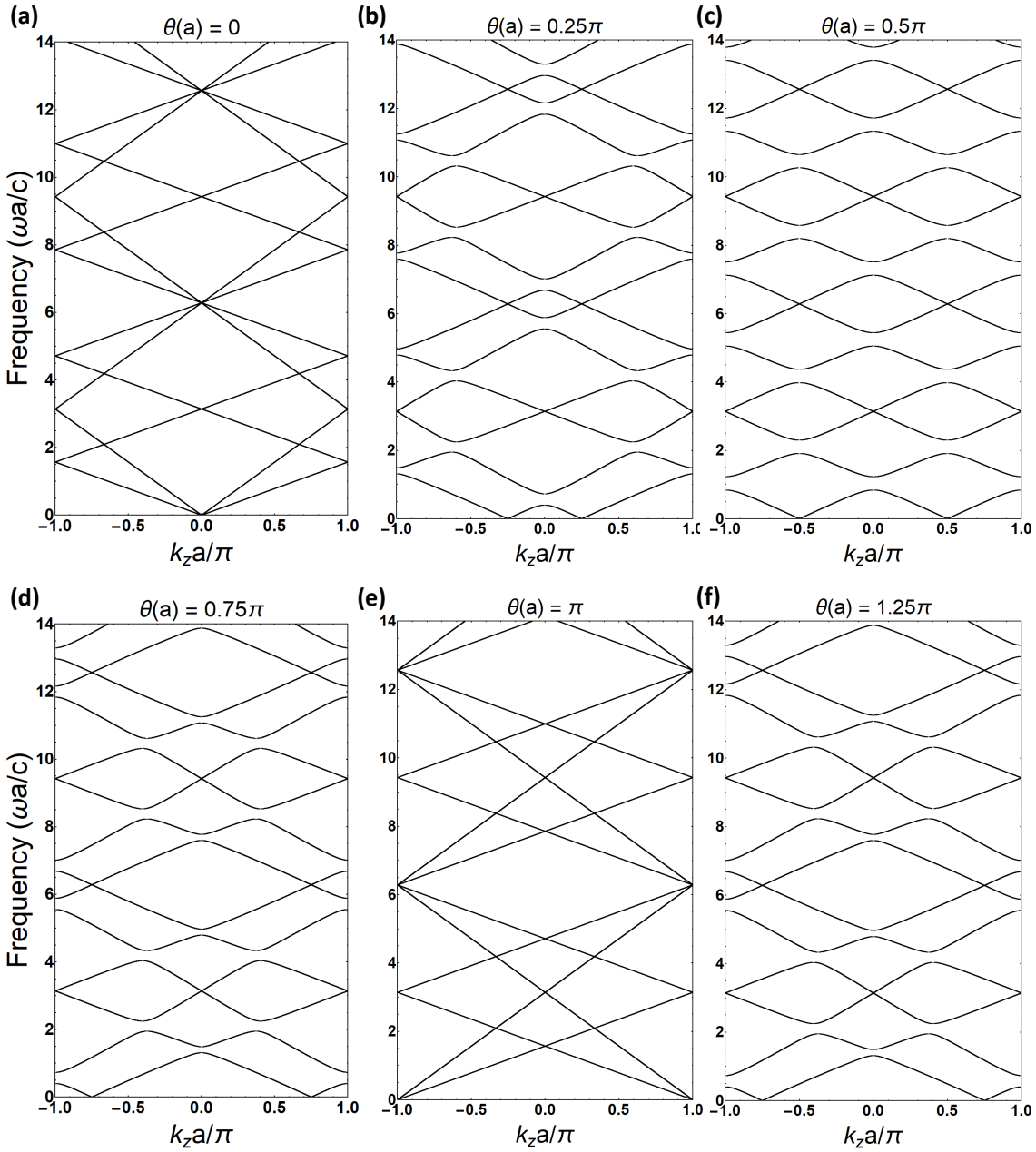

Figure 2.4: The band structures of the chiral photonics crystals. $\theta(a)$ is supposed to be θ_{max}, the maximum value of the structural "twisted" angles. The parameters in the virtual space are given by $\varepsilon'_{11} = 4$ and $\varepsilon'_{22} = \mu'_{11} = \mu'_{22} = 1$, where ε'_{33} can be arbitrary due to $\mathbf{L}(z) = \mathbf{0}$. (a), (b), (c), (d), (e) and (f) are the band structures of $\theta(a)$ equal to 0, 0.25π, 0.5π, 0.75π, π and 1.25π respectively. (a) can overlap with (e) if either one of them is shifted to left or right by 1, so do (b) and (f).

the largest number of complete photonic band gaps.

2.3 Conclusions

In this chapter, the techniques of transformation optics have been applied to reduce 1D isotropic chiral materials to simple anisotropic materials. Because the Maxwell's equations combined with the constitutive relations of two spaces are not invariant, coordinate transformation is not a valid transformation in this situation. By choosing suitable parameters, Oseen transformation can be obtained. Instead of the path of light, optical rotation contributed by chirality can be controlled by the transformation matrix. The transformation method is also valid for other electromagnetic parameters, and other transformation matrix can be obtained so that more chiral media can be designed. The chiral material then acts as a unit cell of a chiral photonic crystal. Since the permittivity and permeability tensors in the physical space consist of unphysical functions, an adjustment to the chirality parameter is made so that a wider frequency range can be considered. By choosing different $\theta(a)$ but fixing $\boldsymbol{\varepsilon}'$ and $\boldsymbol{\mu}'$, the dispersion relations and their properties are examined. The case of $\theta(a) = \pi/2$ will be mainly considered in the following chapters since there appears the largest number of complete photonic band gaps.

Chapter 3

Topological properties of the chiral photonic crystal

Topological photonics has become one of the most famous topics since Haldane and Raghu [11] successfully transferred the topological theories from quantum electronic systems to photonic crystals [10]. The idea has been also confirmed by experimental results [12]. Topological theories of simple anisotropic materials has been widely developed, but the theories of bi-anisotropic media are still an uncharted territory. Due to the coupling of **E** and **H** fields in the constitutive relations, bi-anisotropic materials can provide a wider parameter space for realizing different topological phases [10], for example, the "spin" of photons [19]. In this study, the concept of "spin" of photons is not required, and only the theories of 1D simple isotropic binary photonic crystals are applied. Because of anisotropy and existence of chirality, two independent modes are no longer degenerated. The Zak phases of isolated bands calculated by the coupled modes are discussed in this section; how-

ever, the usages of this type of Zak phase are not widely discussed nowadays. In order to observe the topological properties, by choosing suitable parameters in the virtual space, the eigenstates can be decoupled so that the topological theories of 1D simple isotropic binary photonic crystals can be totally applied. Topological edge states of a system composed of the designed chiral photonic crystal and a simple isotropic binary photonic crystal are also investigated.

3.1 Zak phase

3.1.1 Coupled eigenstates

Zak phase is one of the important topological invariances in 1D photonic systems. The Zak phase of the nth isolated band can be numerically calculated by equation (1.15), where the eigenstates $|\Psi\rangle$ are the eigenvectors obtained in equation (2.13) in principle, and the dual eigenstates $\langle\Psi|$ are the conjugate transpose of the eigenstates $|\Psi\rangle$ although the operator is not Hermitian. The analytical eigenstates of the system will not be discussed because the solutions are too cumbersome. As mentioned in chapter 1, Zak phases can be affected by the position of the origin, and it can be quantized only when a point of symmetry is picked up. Due to existence of chirality and the "spiral" structure, the parity inversion symmetry of the designed chiral photonic crystal is broken. Although the symmetry is still not clear, the Zak phases of the isolated bands can still be quantized by choosing certain positions as

origins. On the basis of the lemma (2.14), the structural "twisted" angle becomes

$$\theta(z) = \begin{cases} \theta_{max}\Big(\frac{z}{a} + \frac{a-d}{a} - \Big\lfloor \frac{z}{a} + \frac{a-d}{a} \Big\rfloor\Big) & , \lfloor (z+a-d)/a \rfloor \in \mathbb{N} \\ \theta_{max} & , \lfloor (z+a-d)/a \rfloor \notin \mathbb{N} \end{cases} \tag{3.1}$$

where d and a are the distance from $\theta(0)$ to θ_{max} and the width of a unit cell respectively. As $\theta(z)$ exists step jumps at $z = d$, the dispersion relation (2.13) should be modified to

$$\begin{aligned} &e^{ik_z a}\mathbf{F}(\omega,0) = \\ &\qquad \mathbf{R}^{-1}(a)\exp\Big(\frac{i\omega a}{c}\big(1-\frac{d}{a}\big)\mathbf{M}'\Big)\mathbf{R}^{-1}(d)\exp\Big(\frac{i\omega a}{c}\big(\frac{d}{a}\big)\mathbf{M}'\Big)\mathbf{R}(0)\mathbf{F}(\omega,0), \end{aligned} \tag{3.2}$$

where $\theta(d) = \theta_{max}$ now. Because the transformation matrix is real and $\mathbf{R}(a) = \mathbf{R}(0)$, the only variable which can affect the Zak phase is d/a if the permittivity and permeability tensors in the virtual space are fixed (see Appendix E). The structures of the chiral photonic crystal, the band structures and the Zak phase of each isolated band with choosing different d/a are shown in Fig. 3.1. The parameters in the virtual space are given by $\varepsilon'_{11} = 4$ and $\varepsilon'_{22} = \mu'_{11} = \mu'_{22} = 1$. $\theta_{max} = \pi/2$ is considered because there appears the largest number of complete photonic band gaps. Figs. 3.1(a), (c), (e) and (g) show the structures of the chiral photonic crystal when d/a respectively equals 1, 0.7, 0.5, 0.3, where red dashed frames indicate the unit cell. The corresponding band structures and the Zak phases of the isolated bands are shown in Figs. 3.1 (b), (d), (f), (h). The band structures are the same because of independence of the positions of origins; however, the Zak phases of the same band are different. Figs. 3.1(b) and (f) show that the Zak phases of all isolated bands can be quantized to π and 0 when $d/a = 1$ and 0.5 respectively. This property is

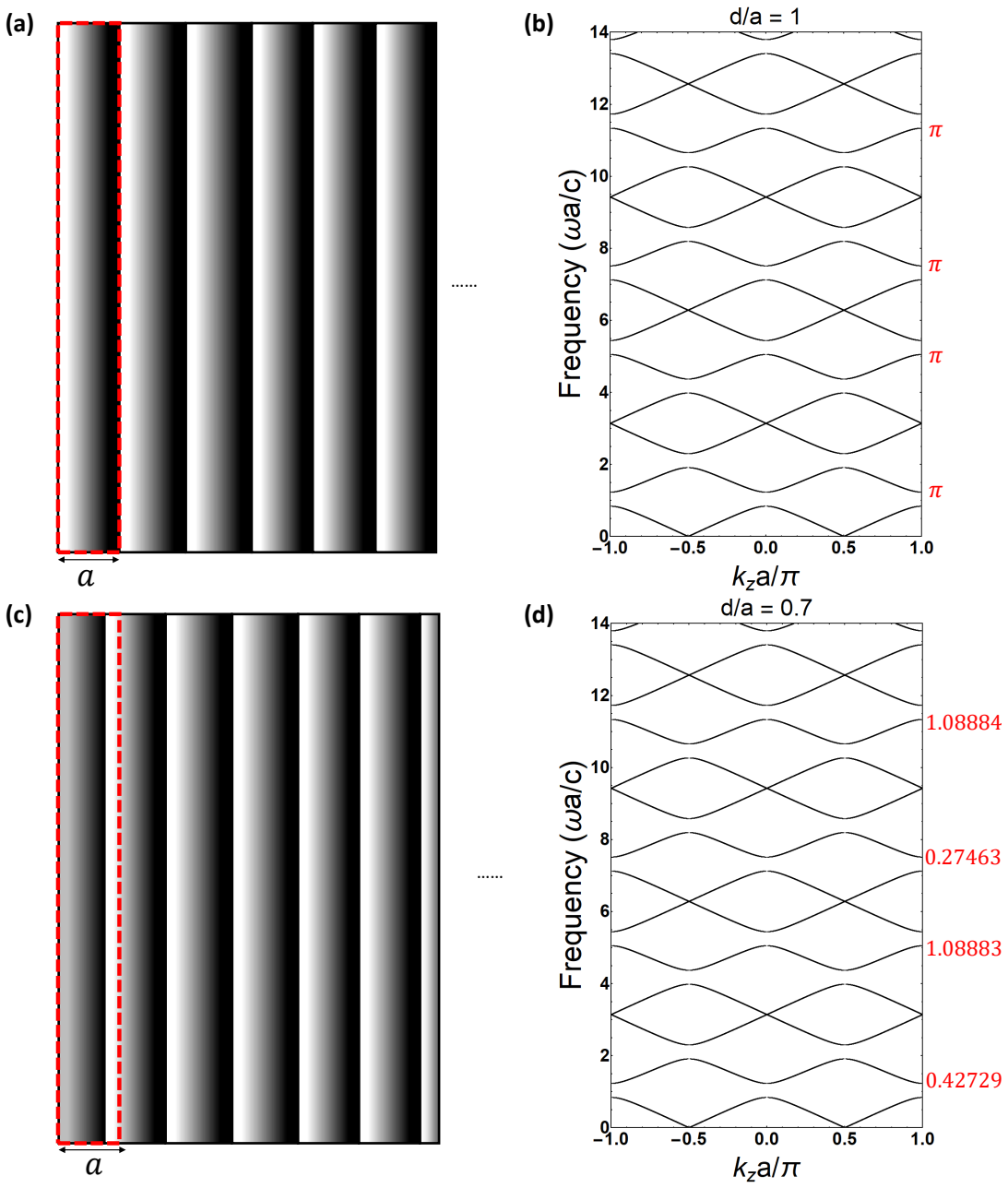
(a)
a
.....
(b)
d/a = 1
Frequency (ωa/c)
$k_z a/\pi$
π
π
π
π
(c)
a
.....
(d)
d/a = 0.7
Frequency (ωa/c)
$k_z a/\pi$
1.08884
0.27463
1.08883
0.42729

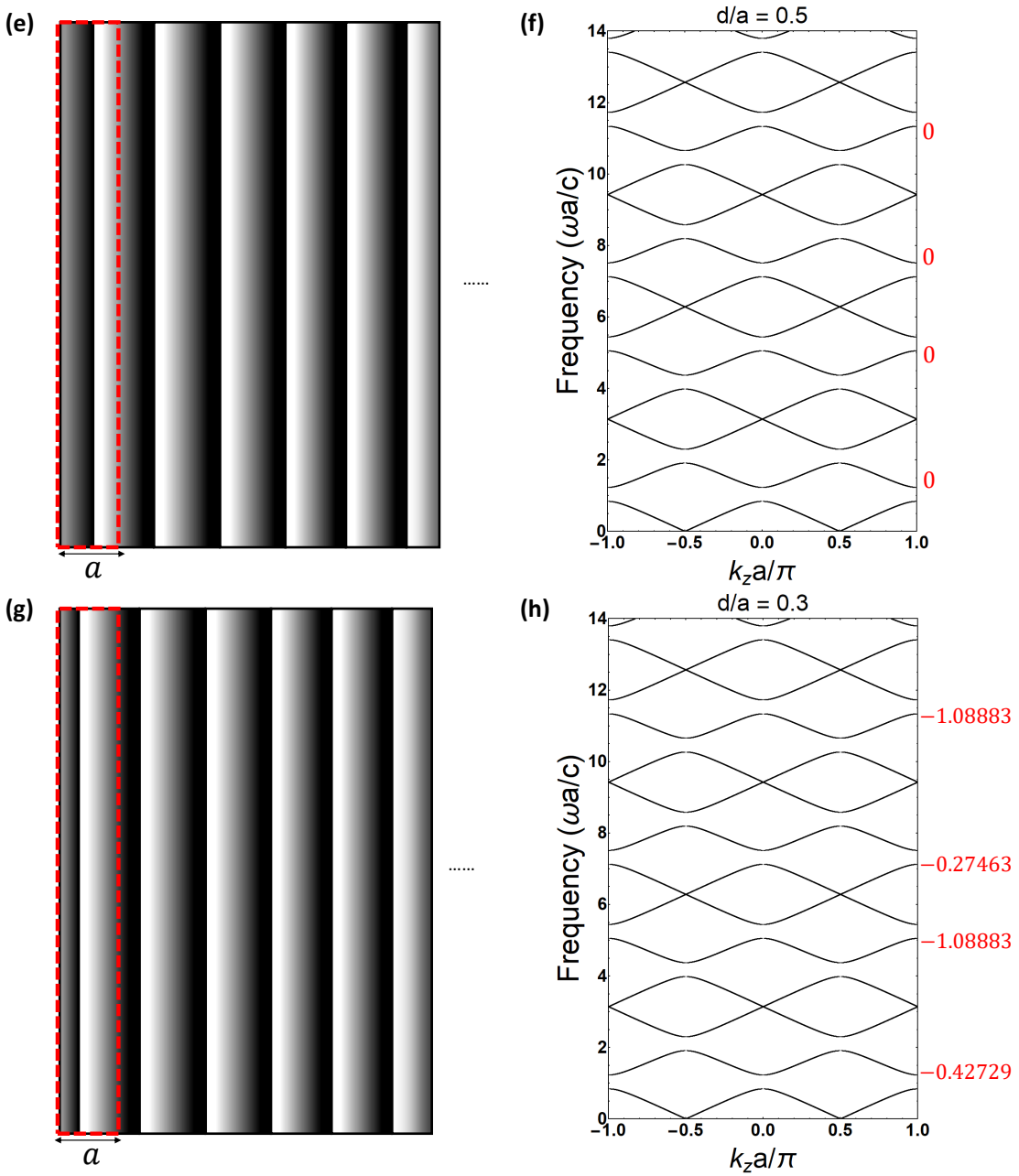

Figure 3.1: (a), (c), (e) and (g) are the same chiral photonic crystal but the methods of choosing a unit cell are different, where $\theta_{max} = \pi/2$. d is the distance from the origin to the point that $\theta(z)$ reaches it first maximum value. Faded colour is used to represent the dielectric parameters are gradually changed along z-direction. (b), (d), (f) and (h) when $\theta(0)$ equals 0, 0.15π, 0.25π and 0.35π respectively. The dielectric and magnetic parameters in the virtual space are given by $\varepsilon'_{11} = 4$ and $\varepsilon'_{22} = \mu'_{11} = \mu'_{22} = 1$. The Zak phases of the isolated bands are labelled near the bands.

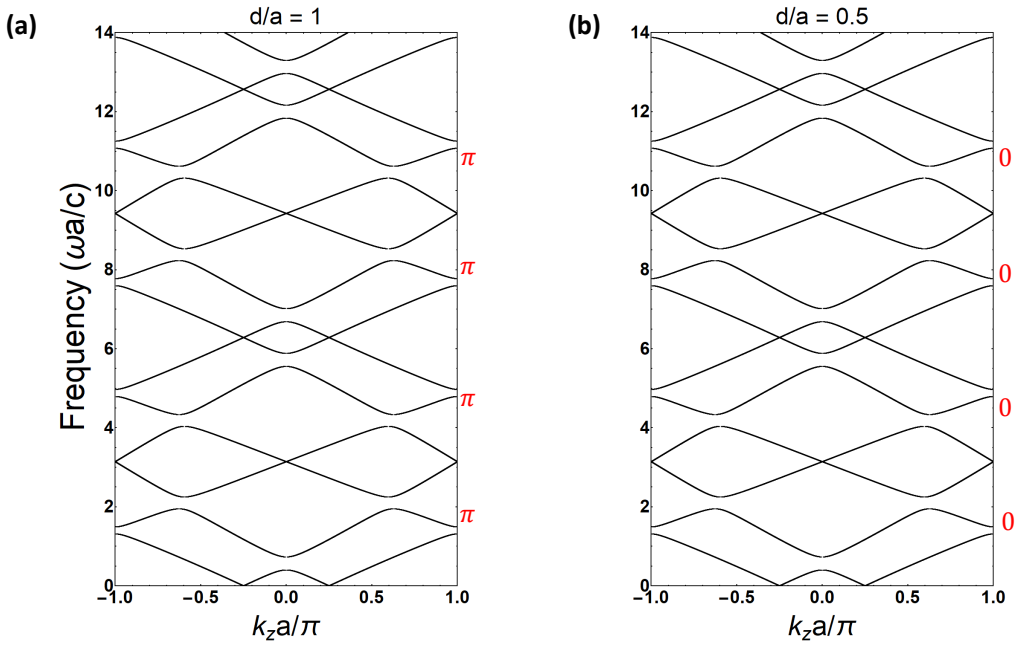

Figure 3.2: (a) and (b) are the band structures calculated by respectively choosing $d/a = 1$ and 0.5 of the chiral photonic crystal with $\theta_{max} = \pi/4$. The Zak phases are labelled near the corresponding isolated bands. The dielectric and magnetic parameters in the virtual space are given by $\varepsilon'_{11} = 4$ and $\varepsilon'_{22} = \mu'_{11} = \mu'_{22} = 1$.

not only valid for this situation. The Zak phases of the isolated bands can also be quantized despite of $\theta_{max} \neq \pi/2$. The band structures of $\theta_{max} = 0.25\pi$ with choosing $d/a = 1$ and 0.5 are shown in Figs. 3.2(a) and (b), where the parameters in the virtual space are given by $\varepsilon'_{11} = 4$ and $\varepsilon'_{22} = \mu'_{11} = \mu'_{22} = 1$. The Zak phases of all isolated bands equal π and 0 when $d/a = 1$ and 0.5 respectively. This can be held even though different parameters in the virtual space are chosen. The case of the permittivity and permeability parameters in the virtual space equal to $\varepsilon'_{11} = 5.2$ and $\varepsilon'_{22} = \mu'_{11} = \mu'_{22} = 1$ is taken to be an example. The band structures with $\theta_{max} = \pi/2$ and the Zak phases are shown in Fig. 3.3. The Zak phases are still equal to π and 0 when $d/a = 1$ and 0.5 respectively. Thus, it is possible to say $d/a = 1$ and $d/a = 0.5$ are the points of symmetry since the Zak phases can be quantized at these points. At this time, the symmetries in the system and the reasons of the Zak phases of all isolated bands equal to π or 0 are still unclear. On the other hand, the Zak phases

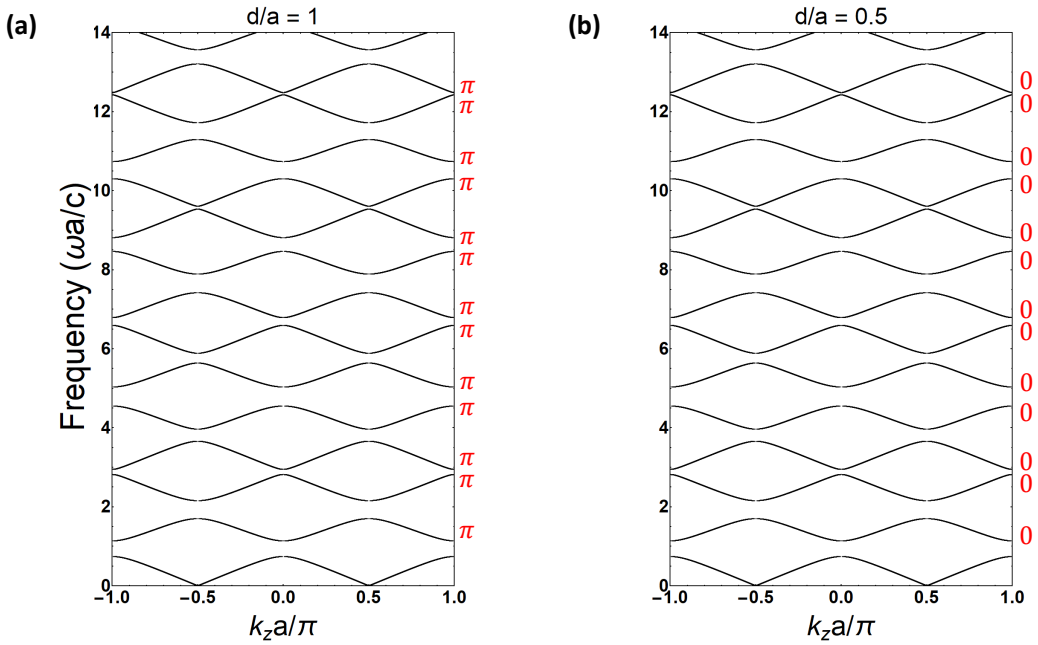

Figure 3.3: (a) and (b) are the band structures calculated by respectively choosing $\theta(0) = 0$ and 0.125π of the chiral photonic crystal with $\theta_{max} = \pi/2$. The Zak phases are labelled near the corresponding isolated bands. The dielectric and magnetic parameters in the virtual space are given by $\varepsilon'_{11} = 5.2$ and $\varepsilon'_{22} = \mu'_{11} = \mu'_{22} = 1$.

calculated by the coupled modes have not been widely discussed nowadays. In order to investigate the topological properties of the chiral photonic crystals, the method of decoupling two modes is explored so that the topological theories developed from 1D simple isotropic binary photonic crystals can be totally applied.

3.1.2 Decoupling two modes

Two independent modes, (E_x, H_y) and (E_y, H_x) modes, are the same in simple isotropic layered photonic crystals, and thereby only either one needs considering (see Appendix F.2). However, (E_x, H_y) and (E_y, H_x) modes are different and even coupled in bi-anisotropic layered photonic crystals. Furthermore, the Zak phases calculated by the coupled eigenmodes have not been widely discussed nowadays. Fortunately, by choosing $\boldsymbol{\varepsilon}'$ and $\boldsymbol{\mu}'$ are both diagonal and $\theta_{max} = \pi/2$, two independent modes of the designed chiral photonic crystal can be decoupled after "second"

Table 3.1: Notation of tensors in the virtual space, physical and transformed structures.

Tensors	Virtual space	Physical structure	Transformed structure
Dielectric	$\boldsymbol{\varepsilon}'(z')$	$\boldsymbol{\varepsilon}(z)$	$\boldsymbol{\varepsilon}''(z)$
Magnetic	$\boldsymbol{\mu}'(z')$	$\boldsymbol{\mu}(z)$	$\boldsymbol{\mu}''(z)$
Chiral	$\mathbf{0}$	$\kappa(z)\mathbf{I}/\omega$	$\mathbf{0}$

transformation such that the topological theories of 1D simple isotropic layered photonic crystals can be totally applied.

Topological invariances can be maintained after continuous deformation. Instead of discontinuous function $\theta(z)$, a similar but a continuous function $\phi(z)$ is considered for "second" transformation, which means the designed chiral photonic crystal undergoes another transformation to become another structure. On the basis of the lemma (2.14), the function can be expressed as

$$\phi(z) = \theta_{max}\frac{z}{a}. \tag{3.3}$$

The transformation matrix is the same as equation (2.7) but $\theta(z)$ is replaced by $\phi(z)$. In order to distinguish the parameters in the physical space and in the transformed structure, the symbols with double primes($''$) are used to emphasize the parameters in the transformed structure. The notation of the tensors in different spaces are shown in Table 3.1. The dielectric permittivity tensor in the transformed structure is

$$\boldsymbol{\varepsilon}''(z) = \frac{1}{\det\mathbf{A}}\mathbf{A}\boldsymbol{\varepsilon}(z)\mathbf{A}^T = \begin{cases} \text{diag}(\varepsilon'_{11}, \varepsilon'_{22}, \varepsilon'_{33}), & \text{if } \lfloor z/a \rfloor \text{ is odd} \\ \text{diag}(\varepsilon'_{22}, \varepsilon'_{11}, \varepsilon'_{33}), & \text{if } \lfloor z/a \rfloor \text{ is even} \end{cases}. \tag{3.4}$$

The magnetic permeability tensor in the transformed structure ($\boldsymbol{\mu}''$) can be found by

simply replacing ε'_{ij} to μ'_{ij}. The chirality parameter κ'' in the transformed structure returns to 0 (see Appendix F.1). From above equation, it is clear that the transformed structure is a simple anisotropic bi-layered structure shown in Fig. 3.4(a), where the permittivity and permeability parameters of white and black slabs are given by equation (3.4) when $\lfloor z/a \rfloor$ is odd and even respectively. In this transformed structure, the width of a unit cell (Λ) is doubled to be $2a$ and z-inversion symmetry exists, where the inversion centers are at the center in each slab. To ensure the Zak phases can be quantized in following calculation, the center of a white slab is chosen as an origin of the system. The dispersion relation can be calculated by transfer-matrix method:

$$e^{ik''_z\Lambda}\mathbf{F}''(\omega,0) = \exp\Big(\frac{i\omega a}{2c}\mathbf{M}''_w\Big)\exp\Big(\frac{i\omega a}{c}\mathbf{M}''_b\Big)\exp\Big(\frac{i\omega a}{2c}\mathbf{M}''_w\Big)\mathbf{F}''(\omega,0), \tag{3.5}$$

where $\mathbf{M}''_w$ and $\mathbf{M}''_b$ are the constant matrices following equation (2.2). The lower indices w and b represent white and black slabs respectively. k''_z is the Bloch wave vector in the transformed structure. The band structure is shown in Fig. 3.4(b), where the parameters in the virtual space are given by $\varepsilon'_{11} = 4$ and $\varepsilon'_{22} = \mu'_{11} = \mu'_{22} = 1$. The band structure shows that two independent eigenmodes are degenerated.

In order to compare the original structure with the transformed structure, two unit cells of the designed chiral photonic crystal are considered as a period ($\Lambda = 2a$) and the center of a unit cells is chosen as an origin of the system. The structure of the chiral photonic crystal and the band structure are shown in Fig. 3.5. The band structure calculated by using single unit cell as a period is already shown in Fig. 2.4(c). Due to double unit cells being regarded as a period, Fig. 3.5(b) can be imagined as the bands in Fig. 2.4(c) folding in the region $k_z a/\pi \in [-0.5, 0.5]$. By

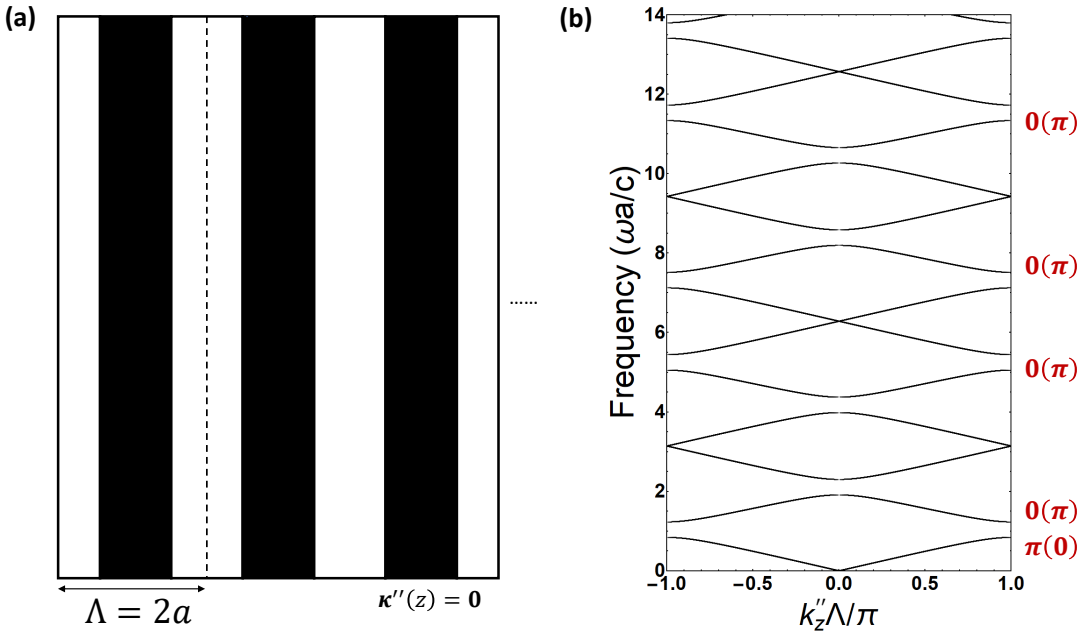

Figure 3.4: (a) The transformed structure, a simple anisotropic binary photonic crystal by choosing $\theta(a) = 0.5\pi$. The permittivity (and permeability) parameters of white and black slabs are given by equation (3.4) when $\lfloor z/a \rfloor$ is odd and even respectively. The center of a white slab is chosen as an origin of the system and the width of a unit cell Λ equals $2a$. (b) The band structure of the transformed anisotropic binary photonic crystal. The permittivity and permeability parameters in the virtual space are given by $\varepsilon'_{11} = 4$ and $\varepsilon'_{22} = \mu'_{11} = \mu'_{22} = 1$. The Zak phases calculated by $|\psi_{x''}\rangle$ ($|\psi_{y''}\rangle$) are labelled near the corresponding isolated bands.

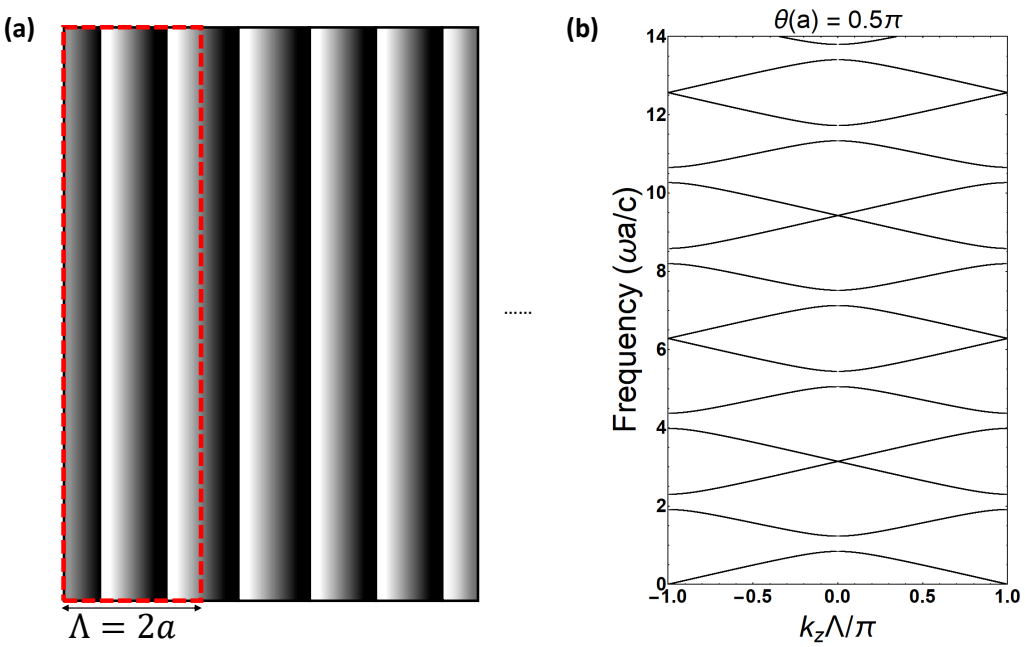

Figure 3.5: (a) The structure of the chiral photonic crystal by choosing $\theta(a) = 0.5\pi$. Two unit cells are regarded as a period and the center of a unit cell is chosen as an origin for fear losing the generality. Faded color is used to represent the parameters are gradually changing along z-direction. (b) The band structure of the chiral photonic crystal by considering 2 unit cells as a period. The permittivity and permeability parameters in the virtual space are given by $\varepsilon'_{11} = 4$ and $\varepsilon'_{22} = \mu'_{11} = \mu'_{22} = 1$.

comparing Fig. 3.4(b) with Fig. 3.5(b), the band structures can be overlapped by shifting either one to the left (or right) by 1. i.e.,

$$\frac{k_z\Lambda}{\pi} = \frac{k_z''\Lambda}{\pi} + (2s-1), \tag{3.6}$$

where s is an integer for controlling the normalized wave vector within the region $[-1, 1]$. The eigenstate at $k_z\Lambda/\pi$ (in original structure) is the same as at $k_z''\Lambda/\pi + (2s-1)$ (in transformed structure) (see Appendix F.3). Therefore, the Zak phases of the corresponding bands in two band structures are the same. If the eigenvectors are rearranged in the from $\mathbf{F}'' = \left(E_{x''}''\ Z_0H_{y''}''\ E_{y''}''\ -Z_0H_{x''}''\right)^T$, the operator in equation (3.5) becomes a block-diagonal matrix, which is composed of two 2×2 matrices. In other words, the eigenstates in the transformed structure can be decoupled to $(E_{x''}''\ Z_0H_{y''}'')^T$ and $(E_{y''}''\ -Z_0H_{x''}'')^T$, which are denoted as $|\psi_{x''}\rangle$ and $|\psi_{y''}\rangle$ respectively for clear presentation. Similarly, $|\psi_x\rangle$ and $|\psi_y\rangle$ will be used to represent the same modes in the original structure.

In simple isotropic layered photonic crystals, only either one of the modes needs considering because $|\psi_x\rangle$ is equivalent to $|\psi_y\rangle$. However, in simple anisotropic binary layered photonic crystals, both of them have to be considered since $|\psi_x\rangle$ is not equivalent to $|\psi_y\rangle$. If $|\psi_{x''}\rangle$ (or $|\psi_{y''}\rangle$) mode is considered only, the transformed structure can be further regarded as a simple isotropic AB (or BA) layered photonic crystal, where the parameters are given by $\varepsilon_A = \varepsilon_{11}'$, $\varepsilon_B = \varepsilon_{22}'$, $\mu_A = \mu_{22}'$ and $\mu_B = \mu_{11}'$. Thus, the topological theories of simple isotropic binary photonic crystals can be totally applied. The inversion centers of binary photonic crystal are at the center of each slab. For example, in Fig. 3.5(a), the inversion centers are at the

center of each white and black slabs. In simple isotropic binary photonic crystal, if the Zak phase of an isolated band is $0(\pi)$ by choosing one of the inversion centers as an origin, the Zak phase of the same band must be $\pi(0)$ when another inversion center is chosen [35]. Consequently, in my transformed simple anisotropic binary photonic crystal, if the Zak phase calculated by $|\psi_{x''}\rangle$ mode is $0(\pi)$, the Zak phase of the same band calculated by $|\psi_{y''}\rangle$ mode will be $\pi(0)$. In other words, one isolated band has two different quantized Zak phases. The Zak phases of the bands are also shown in Fig. 3.4(b).

3.2 Existence of interface states

The idea of "second transformation" has been introduced in previous section. When $|\psi_{x''}\rangle$ or $|\psi_{y''}\rangle$ mode is considered, the transformed structure can be regarded as a simple isotropic AB or BA layered structure respectively. Hence, the topological theories of simple isotropic binary photonic crystals can be totally applied. In this section, topological edge states of a system composed of my chiral photonic crystal and a simple isotropic binary photonic crystal are going to investigated. In order to guarantee the mid-gap positions of the photonic crystals are the same, the optical path lengths should be equivalent [35, 36]. i.e.,

$$(\sqrt{\varepsilon'_{11}} + \sqrt{\varepsilon'_{22}})a = n_A d_A + n_B d_B, \tag{3.7}$$

where n_A and n_B are the refractive indices of the slabs A and B; d_A and d_B are the widths of slabs A and B respectively. Without loss of generality, the method of choosing a unit cell is the same as Figs. 3.4(a) and 3.5(a). The system is composed

of 20 unit cells of my chiral photonic crystal on the left and 10 unit cells of a simple isotropic binary photonic crystal on the right. The widths of unit cells of my chiral photonic crystal and the simple isotropic binary photonic crystal are a and $2a$ respectively. The transmission spectra of the system calculated by $|\psi_x\rangle$ and $|\psi_y\rangle$ are shown in Figs. 3.6(a) and (b) respectively. The parameters of the chiral photonic crystal in the virtual space are given by $\varepsilon'_{11} = 3.23$ and $\varepsilon'_{22} = \mu'_{11} = \mu'_{22} = 1$, and the parameters of the simple isotropic binary photonic crystal are given by $\varepsilon_A = 4.2$ and $\varepsilon_B = \mu_A = \mu_B = 1$. The transmission spectra are the same and interface states appear in the 1st, 3rd, 5th, 7th, 8th, 10th, 11th and 12th gaps. The reason of the same transmission spectra can be explained by the transformed anisotropic binary photonic crystal, and the positions of interface states can also be predicted. Although the permittivity and permeability tensors in the original structure are complicated, there is a conformal mapping to the transformed structure. Therefore, the system can be regraded as a composition of 10 unit cells of the transformed anisotropic binary photonic crystal on the left and 10 unit cells of the simple isotropic binary photonic crystal on the right. Since a center of a unit cell has been chosen as an origin, the incident fields $|\psi_x\rangle$ or $|\psi_y\rangle$ can always be decomposed into a linear combination of $|\psi_{x''}\rangle$ and $|\psi_{y''}\rangle$. Consequently, the transmission spectrum of $|\psi_x\rangle$ or $|\psi_y\rangle$ is the sum of the transmission spectra of $|\psi_{x''}\rangle$ and $|\psi_{y''}\rangle$, which is the reason why the transmission spectra are the same. Second, the transformed anisotropic binary photonic crystal can be further regarded as a simple isotropic binary photonic crystal when either $|\psi_{x''}\rangle$ or $|\psi_{y''}\rangle$ mode is considered; thus, the system can be further regarded as a composition of 10 unit cells of a simple isotropic binary photonic crystal on the left and 10 unit cells of

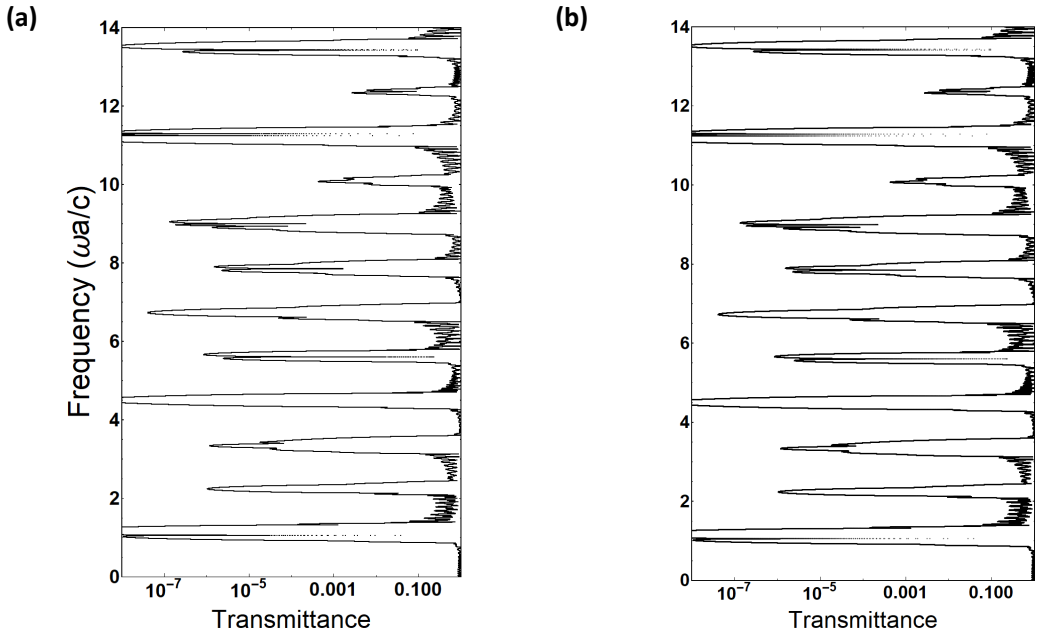

Figure 3.6: The transmission spectra of a system composed of 20 unit cells of my designed chiral photonic crystal on the left side and 10 unit cells of the simple isotropic binary photonic crystal on the right side. The parameters of the chiral photonic crystal in the virtual space are given by $\varepsilon'_{11} = 3.23$ and $\varepsilon'_{22} = \mu'_{11} = \mu'_{22} = 1$. The parameters of the simple isotropic binary photonic crystal are given by $\varepsilon_A = 4.2$, $\varepsilon_B = \mu_A = \mu_B = 1$ and $d_A = 0.76a$ and $d_B = 1.24a$. (a) and (b) are the transmission spectra of $|\psi_x\rangle$ and $|\psi_y\rangle$ modes respectively, where the spectra are the same.

a simple isotropic binary photonic crystal on the right. The existence of interface states of a system composed of two simple isotropic binary photonic crystals can be predicted by the signs of the surface impedance $\zeta^{(n)}$. Interface states appear when $\mathrm{sgn}\left[\zeta^{(n)}\right]$ of two connected photonic crystals are opposite in a common gap. The transmission spectra calculated by $|\psi_{x''}\rangle$ and $|\psi_{y''}\rangle$ are shown in Figs. 3.7(a) and (d). The band structures of the transformed anisotropic binary and simple isotropic binary photonic crystals are shown in (b) and (e) (also in (e) and (f)) respectively. The parameters of the anisotropic binary photonic crystal and of the simple isotropic binary photonic crystal are the parameters used in Fig. 3.6. The band structures shown in Figs. 3.7(b) and (e) are the same but the Zak phases are different by π. Magenta strip represents $\mathrm{sgn}\left[\zeta^{(n)}\right] > 0$; otherwise, the strip is cyan. The interface state exists if $\mathrm{sgn}[\zeta^{(n)}]$ in a common gap are opposite. In Fig. 3.7(a), the interface states exist in the 5th , 7th, 8th, 10th, 11th and 12th gaps; in Fig. 3.7(d), the interface states exist in 1st, 3rd, 8th, 10th and 12th gaps. Therefore, in the transmission spectrum of $|\psi_x\rangle$ or $|\psi_y\rangle$ mode, interface states of a system composed of my designed chiral photonic crystal and the simple isotropic binary photonic crystal will exist in the 1st, 3rd, 5th, 7th, 8th, 10th, 11th and 12th gaps. The prediction is consistent with the transmission spectra shown in Fig. 3.6.

3.3 Conclusions

In this chapter, some topological features of my designed chiral photonic crystal are discussed. Because of anisotropy and existence of chirality, two independent eigenstates, (E_x, H_y) and (E_y, H_x) modes, are no longer degenerated and even coupled. The Zak phases calculated by the coupled eigenstates has been investigated.

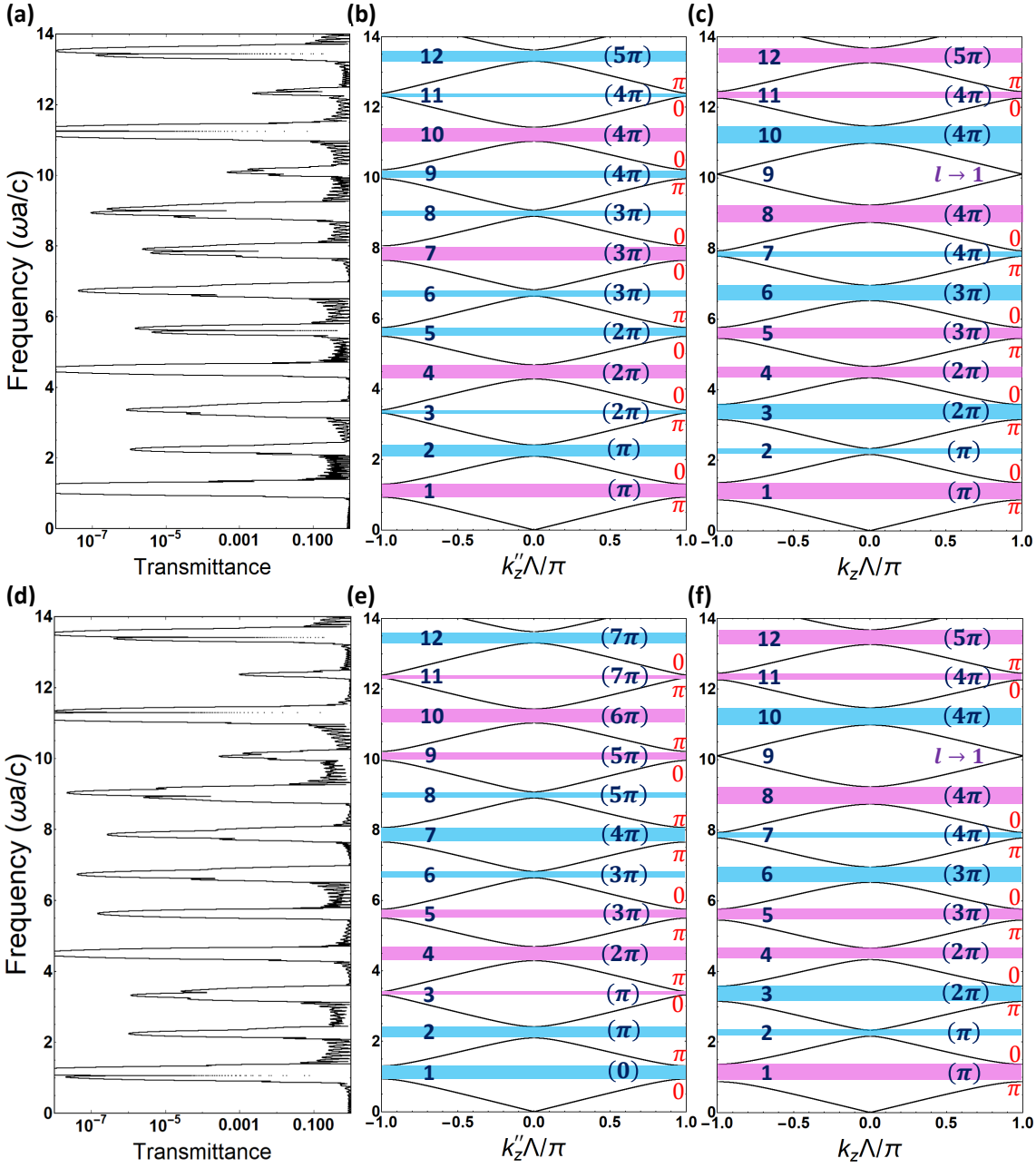

Figure 3.7: (a) and (d) are the transmission spectra calculated by $|\psi_x\rangle$ and $|\psi_y\rangle$ modes respectively. The system is composed of 10 unit cells of the transformed anisotropic binary photonic crystal on the left and 10 unit cells of the simple isotropic binary photonic crystal on the right. The parameters in the virtual space are given by $\varepsilon'_{11} = 3.23$ and $\varepsilon'_{22} = \mu'_{11} = \mu'_{22} = 1$, and the parameters of the simple isotropic binary photonic crystal are given by $\varepsilon_A = 4.2$, $\varepsilon_B = \mu_A = \mu_B = 1$ and $d_A = 0.76a$ and $d_B = 1.24a$. (b) and (e) are the band structures of the transformed anisotropic binary photonic crystal, and (c) and (f) are the band structure of the simple isotropic binary photonic crystal. In both band structures, the magenta and cyan strips represent the gaps with $\zeta > 0$ and $\zeta < 0$ respectively. The Zak phase of each band are labelled near the band and the number in the brackets are the sum of the Zak phases below the gaps.

The Zak phases of all isolated bands can be quantized to π and 0 when the $d/a = 1$ and 0.5 respectively. Because the symmetries in the system and the usages of these Zak phases are still unknown at this time, the method of decoupling two independent modes is introduced. By choosing diagonal $\boldsymbol{\varepsilon}'$ and $\boldsymbol{\mu}'$ and $\theta_{max} = \pi/2$, the chiral photonic crystal can "secondly" transform to an simple anisotropic binary photonic crystal, in which parity inversion symmetry appears. If either (E''_x, H''_y) or (E''_y, H''_x) is considered, the transformed structures can be further regarded as a simple isotropic AB or BA layered structure respectively. Hence, the topological theories of simple isotropic binary photonic crystals can be totally applied. Different from simple isotropic layered structures, one isolated band contains two different quantized Zak phases (0 and π). Furthermore, topological edge states of a system composed of 20 unit cells of my chiral photonic crystal and 10 unit cells of a simple isotropic binary photonic crystal has been examined. Because (E_x, H_y) and (E_y, H_x) modes can be decomposed in terms of (E''_x, H''_y) and (E''_y, H''_x), the positions of interface states of a system composed of the chiral photonic crystal and a simple isotropic binary photonic crystal is the sum of the positions of (a) a system composed of 10 unit cells of the transformed AB isotropic binary photonic crystal and 10 unit cells of a simple isotropic binary photonic crystal and (b) a system composed of 10 unit cells of the transformed BA isotropic binary photonic crystal and 10 unit cells of a simple isotropic binary photonic crystal.

Chapter 4

Summary

Transformation optics is a useful theory for giving more information of permittivity and permeability parameters to guide the paths of light in materials for achieving certain phenomena. The ideas are based on the invariances of Maxwell's equations and Helmholz equation under coordinate transformation so that there is a conformal or quasi-conformal mapping between two spaces. Because of difference of constitutive relations between simple and bi-anisotropic media, other transformation matrix should be considered in order to eliminate the chirality parameters. A chiral photonic crystal can be composed of repeating the designed chiral material. Some physical properties of the designed photonic crystals are also examined.

In chapter 1, the concepts of chiral materials, mathematical foundation of transformation optics and the topological theories of 1D photonic systems are briefly reviewed. Chiral materials are composed of the particles which cannot superimposed on their mirror images. The properties of natural optical activities occurred in chiral materials are attractive in topological photonics since a wider parameter space can

be provided for realization of different topological phases. Second, the foundation of transformation optics and the general idea of transformation between simple and chiral media are also introduced. Because of different constitutive relations between simple and chiral media, other transformation methods need considering instead of coordinate transformation. Finally, the topology related to this study are reviewed. Zak phases of isolated bands can be numerically found by the summation of all inner products of the neighbouring eigenstates, and they can even be quantized to 0 or π if a point of symmetry is picked up. The theory for predicting topological edge states of a system composed of two simple isotropic binary photonic crystals has also been reviewed.

In chapter 2, the details of transforming 1D anisotropic medium with isotropic chirality to 1D simple anisotropic medium is discussed. The transformation function $\theta(\omega, z)$ can be easily obtained by choosing suitable permittivity and permeability tensors. The transformation matrix is a rotation matrix along the axis of propagation. Instead of the trajectory, optical rotation attributed to chirality can be controlled by the transformation matrix. In order that the analytical wave solution is available for a wider frequency range, the chirality parameter is adjusted to $\kappa(\omega, z) \rightarrow \kappa_0(z)/\omega$. The band structures of the chiral photonic crystals with different structural angles $\theta(a)$ are examined.

In chapter 3, some topological features of the chiral photonic crystal are investigated. Because of anisotropy and existence of chirality, two independent eigenmodes, (E_x, H_y) and (E_y, H_x), are no longer degenerated and even coupled. The Zak phases of isolated bands calculated by these coupled eigenstates are examined. Although the symmetry in the designed chiral photonic crystal is still unclear, the

Zak phases can still be quantized when certain positions are chosen as origins. In order to observe the topological features, the method of decoupling two modes is explored. By choosing diagonal permittivity and permeability tensors in the virtual space and $\theta_{max} = \pi/2$, the chiral photonic crystal can "secondly" transform to a simple anisotropic binary photonic crystal. Furthermore, it can even be regarded as simple isotropic AB and BA photonic crystals if $(E''_{x''}\ Z_0 H''_{y''})^T$ and $(E''_{y''}\ -Z_0 H''_{x''})^T$ modes are considered individually. Therefore, the topological theories of 1D simple isotropic binary photonic crystals can be totally applied. The interface states of a system composed of my chiral photonic crystal and a simple isotropic binary photonic crystal are also examined.

In this thesis, the electromagnetic tensors in the physical space are simplified so that the Oseen transformation is obtained. If more general chirality tensor or $\mathbf{L}(\omega, z)$ is taken into consideration, the transformation will become more complicated and more systems can be designed. Furthermore, the parameters in the virtual space are not necessarily physical so that more systems can be designed. The techniques (Appendix B) can actually be generalized to 3-dimensional systems; however, the processes will be totally different and more complicated due to tackling the complicated tensorial differential equations.

Appendix A

Mathematical foundation of transformation optics

A.1 Transformation of electromagnetic fields

The main idea of transformation optics is to control the paths of light. The propagation direction of EM waves can take use of the direction of Poynting vector **S**. Instead of considering the transformation of electric and magnetic fields, the transformation of the Poynting vector is first considered. Because the Poynting vector is a pseudovector, the transformation should be

$$\mathbf{S}' = a\mathbf{A}\mathbf{S} \;\mapsto\; S'^{\,\alpha} = aA^{\alpha}_{\ i}\, S^{i}, \tag{A.1}$$

where **A** is a Jacobian matrix with components $A^{\alpha}_{\ i} = \partial x'^{\,\alpha}/\partial x^{i}$ and summation convention is implied. Greek symbols are also equal to $1, 2, 3$. The coefficient a is inserted in the equation due to the transformation rule of pesudovectors. Originally a

is defined by the transformation matrix of polar vectors, but now the transformation matrix of polar vectors is unknown and thus a cannot be well defined in this moment. Suppose the unknown transformation matrix of $\mathbf{E}$ and $\mathbf{H}$ is $\mathbf{J}$. The cross product of the electric and magnetic fields are

$$\mathbf{E}' \times \mathbf{H}' \doteq \epsilon^{\alpha\beta\gamma} E'_{\ \beta} H'_{\ \gamma} = \epsilon^{\alpha\beta\gamma} J_{\beta}^{\ i} E_i J_{\gamma}^{\ j} H_j, \tag{A.2}$$

where $\epsilon^{\alpha\beta\gamma}$ is the Levi-Civita symbol. By combining the above equations and multiplying $J_{\alpha}^{\ k}$ on both sides, it becomes

$$aJ_{\alpha}^{\ k} A^{\alpha}_{\ i} S^i = \epsilon^{\alpha\beta\gamma} J_{\alpha}^{\ k} J_{\beta}^{\ i} J_{\gamma}^{\ j} E_i H_j = (\mathrm{det}\mathbf{J}) \epsilon^{kij} E_i H_j$$

Therefore,

$$a\mathbf{J}^T\mathbf{A} = (\mathrm{det}\mathbf{J})\mathbf{I} \Rightarrow \mathbf{J} = (\mathbf{A}^{-1})^T = (\mathbf{A}^T)^{-1} \text{ and } a = \frac{1}{\mathrm{det}\mathbf{A}}, \tag{A.3}$$

where $\mathbf{I}$ is an identity matrix. In this process, we can understand the transformation is corresponding to covariant transformations of electric and magnetic fields.

A.2 Invariance of Maxwell's equations under coordinate transformation

In original space, the Faraday' s law in a simple medium can be expressed as

$$\boldsymbol{\nabla} \times \mathbf{E} = -i\omega\boldsymbol{\mu}\mathbf{H} \ \mapsto \ \epsilon^{ijk}\partial_j E_k = -i\omega\mu^{ij} H_j. \tag{A.4}$$

By mapping the spaces from $\mathbf{x}$ to $\mathbf{x}'$, the transformations of polar vectors ($\mathbf{E}$ and $\mathbf{H}$) are

$$E'_{\alpha} = \left[(\mathbf{A}^T)^{-1}\right]_i^{\ j} E_j,\ H'_{\alpha} = \left[(\mathbf{A}^T)^{-1}\right]_{\alpha}^{\ j} H_i, \tag{A.5}$$

where $\mathbf{A}$ is a Jacobian matrix with the following relations

$$A^{\alpha}_{\ i} = \frac{\partial x'^{\alpha}}{\partial x^i} \equiv \partial_i x'^{\alpha},\ [\mathbf{A}^{-1}]^i_{\ \alpha} = \frac{\partial x^i}{\partial x'^{\alpha}} \equiv \partial'_{\alpha} x^i. \tag{A.6}$$

By substituting (A.5) to (A.4), left-hand side of the equation should be

$$\epsilon^{ijk}\partial_j E_k = \epsilon^{ijk}\partial_j (A^{\alpha}_{\ k} E'_{\alpha}) = \epsilon^{ijk}\left[(\partial_j \partial_k x'^{\alpha})E'_{\alpha} + (\partial_k x'^{\alpha})\partial_j E'^{\alpha}\right],$$

The first term in the bracket is vanished by swapping the dummy indices j and k. Therefore,

$$\epsilon^{ijk}\partial_k x'^{\alpha}\partial_j E'_{\alpha} = \epsilon^{ijk}\partial_k x'^{\alpha}\partial_j x'^{\beta}\partial'_{\beta} E'_{\alpha} = -i\omega\mu^{ij}\partial_j x'^{\alpha} H'_{\alpha},$$

and after multiplying $\partial_i x'^{\gamma}$ on both sides, we get

$$\epsilon^{ijk}\partial_i x'^{\gamma}\partial_k x'^{\alpha}\partial_j x'^{\beta}\partial'_{\beta} E'_{\alpha} = -i\omega\partial_i x'^{\gamma}\mu^{ij}\partial_j x'^{\alpha} H'_{\alpha} = -i\omega A^{\gamma}_{\ i}\mu^{ij} A^{\alpha}_{\ j} H'_{\alpha}. \tag{A.7}$$

Because of

$$\epsilon^{ijk}\partial_i x'^{\gamma}\partial_k x'^{\alpha}\partial_j x'^{\beta} = \epsilon^{\gamma\alpha\beta}(\det\mathbf{A}), \tag{A.8}$$

we get

$$\epsilon^{\gamma\alpha\beta}(\det\mathbf{A})\partial'_{\beta} E'_{\alpha} = -i\omega A^{\gamma}_{\ i}\mu^{ij} A^{\alpha}_{\ j} H'_{\alpha} \Rightarrow \nabla' \times \mathbf{E}'(\mathbf{x}') = -i\omega\boldsymbol{\mu}'(\mathbf{x}')\mathbf{H}'(\mathbf{x}') \tag{A.9}$$

if I assume

$$\boldsymbol{\mu}'(\mathbf{x}') = \frac{\mathbf{A}\boldsymbol{\mu}(\mathbf{x})\mathbf{A}^T}{\det\mathbf{A}}. \tag{A.10}$$

It is easy to prove that Ampere' s law is also invariant under coordinate transformation, and the permittivity tensor is

$$\boldsymbol{\varepsilon}'(\mathbf{x}') = \frac{\mathbf{A}\boldsymbol{\varepsilon}(\mathbf{x})\mathbf{A}^T}{\det\mathbf{A}}. \tag{A.11}$$

.

Appendix B

Raising chirality via non-coordinate transformation

In chiral medium, one of the Maxwell's equations combined with the constitutive relation is

$$\begin{aligned} &\boldsymbol{\nabla} \times \mathbf{E}(\mathbf{x}) - \omega\sqrt{\varepsilon_0\mu_0}\,\boldsymbol{\kappa}(\mathbf{x})\mathbf{E}(\mathbf{x}) = -i\omega\boldsymbol{\mu}(\mathbf{x})\mathbf{H}(\mathbf{x}) \\ &\mapsto \epsilon^{ijk}\partial_j E_k - \omega\sqrt{\varepsilon_0\mu_0}\kappa^{ij}E_j = -i\omega\mu^{ij}H_j. \end{aligned} \tag{B.1}$$

The aim is to transform a chiral medium to a simple medium, so the Faraday's law in transformed space should be

$$\nabla' \times \mathbf{E}'(\mathbf{x}') = -i\omega\boldsymbol{\mu}'(\mathbf{x}')\mathbf{H}'(\mathbf{x}') \;\mapsto\; \epsilon^{\alpha\beta\gamma}\partial'_\beta E'_\gamma = -i\omega\mu'^{\,\alpha\beta}H'_\beta \tag{B.2}$$

Due to the invariance of Maxwell's equations under coordinate transformation, other transformation matrix $\mathbf{A}$ should be found in order to eliminate the chirality. i.e.,

$A^{\alpha}_{\ i} \neq \partial x'^{\alpha}/\partial x^i$. The transformation of polar vectors is supposed to be the same as equation (A.5) for consistency. By substituting equation (A.5) into equation (B.1), we get

$$\begin{aligned}\epsilon^{ijk}\partial_j E_k - \omega\sqrt{\varepsilon_0\mu_0}\kappa^{ij}E_j &= \epsilon^{ijk}\partial_j(A^{\alpha}_{\ k}E'_{\alpha}) - \omega\sqrt{\varepsilon_0\mu_0}\kappa^{ij}A^{\alpha}_{\ j}E'_{\alpha} \\ &= \epsilon^{ijk}\big[(\partial_j A^{\alpha}_{\ k})E'_{\alpha} + A^{\alpha}_{\ k}\partial_j E'_{\alpha}\big] - \omega\sqrt{\varepsilon_0\mu_0}\kappa^{ij}A^{\alpha}_{\ j}E'_{\alpha} \\ &= -i\omega\mu^{ij}A^{\alpha}_{\ j}H'_{\alpha}.\end{aligned}$$

If $\epsilon^{ijk}[(\partial_j A^{\alpha}_{\ k})E'_{\alpha}] - \omega\sqrt{\varepsilon_0\mu_0}\kappa^{ij}A^{\alpha}_{\ j}E'_{\alpha} = 0$, the equation becomes

$$\epsilon^{ijk}A^{\alpha}_{\ k}\partial_j E'_{\alpha} = -i\omega\mu^{ij}A^{\alpha}_{\ j}H'_{\alpha} \tag{B.3}$$

In Appendix A, chain rule is applied such that the partial derivative can change from $\boldsymbol{\partial}$ to $\boldsymbol{\partial}'$. i.e.

$$\frac{\partial E'^{\alpha}}{\partial x^j} = \frac{\partial x'^{\beta}}{\partial x^j}\frac{\partial E'^{\alpha}}{\partial x'^{\beta}} = A^{\beta}_{\ j}\frac{\partial}{\partial x'^{\beta}}E'_{\alpha}.$$

Therefore, it is possible to regard the transformation of the derivative as $\partial_j = A^{\beta}_{\ j}\partial'_{\beta}$ in coordinate transformation. If the same idea is drawn and applied in my transformation, equation (B.3) becomes

$$\begin{aligned}\epsilon^{ijk}A^{\alpha}_{\ k}A^{\beta}_{\ j}\partial'_{\beta}E'_{\alpha} &= -i\omega\mu^{ij}A^{\alpha}_{\ j}H'_{\alpha} \\ \epsilon^{ijk}A^{\gamma}_{\ i}A^{\alpha}_{\ k}A^{\beta}_{\ j}\partial'_{\beta}E'_{\alpha} &= -i\omega A^{\gamma}_{\ i}\mu^{ij}A^{\alpha}_{\ j}H'_{\alpha} \\ \epsilon^{\gamma\beta\alpha}(\det\mathbf{A})\partial'_{\beta}E'_{\alpha} &= -i\omega A^{\gamma}_{\ i}\mu^{ij}A^{\alpha}_{\ j}H'_{\alpha}\end{aligned}$$

$$\Rightarrow\ \boldsymbol{\mu}'(\mathbf{x}') = \frac{\mathbf{A}\boldsymbol{\mu}(\mathbf{x})\mathbf{A}^T}{\det\mathbf{A}}. \tag{B.4}$$

Although $\mathbf{A}$ is not a Jacobian matrix, the transformation law of tensors are still valid; however, we should be more careful that another Maxwell's equation have not yet been considered, which is

$$\begin{aligned} \boldsymbol{\nabla} \times \mathbf{H}(\mathbf{x}) - \omega\sqrt{\varepsilon_0\mu_0}\,\boldsymbol{\kappa}^T(\mathbf{x})\mathbf{H}(\mathbf{x}) &= i\omega\boldsymbol{\varepsilon}(\mathbf{x})\mathbf{E}(\mathbf{x}) \\ \mapsto \epsilon^{ijk}\partial_j H_k - \omega\sqrt{\varepsilon_0\mu_0}\kappa^{ji}E_j &= i\omega\varepsilon^{ij}E_j \end{aligned} . \tag{B.5}$$

If the same procedures are followed, the condition of the transformation matrix is $\epsilon^{ijk}[(\partial_j A^{\alpha}{}_{k})H'_{\alpha}] - \omega\sqrt{\varepsilon_0\mu_0}\kappa^{ji}A^{\alpha}{}_{j}H'_{\alpha} = 0$, which contradicts with the condition stated above, $\epsilon^{ijk}[(\partial_j A^{\alpha}{}_{k})E'_{\alpha}] - \omega\sqrt{\varepsilon_0\mu_0}\kappa^{ij}A^{\alpha}{}_{j}E'_{\alpha} = 0$. To resolve this contradiction, different transformations of $\mathbf{E}$ and $\mathbf{H}$ are applied. Noted that the transformation is not limited in coordinate transformation, so the freedom of choosing the transformation is more flexible. i.e.

$$\mathbf{E}' = (\boldsymbol{\mathcal{A}}^T)^{-1}\mathbf{E}, \;\; \mathbf{H}' = (\boldsymbol{\mathcal{B}}^T)^{-1}\mathbf{H}, \tag{B.6}$$

where $\boldsymbol{\mathcal{A}}$ and $\boldsymbol{\mathcal{B}}$ are the transformation matrices. The conditions of the transformation matrices become

$$\begin{cases} \epsilon^{ijk}[(\partial_j \mathcal{A}^{\alpha}{}_{k})E'_{\alpha}] - \omega\sqrt{\varepsilon_0\mu_0}\kappa^{ij}\mathcal{A}^{\alpha}{}_{j}E'_{\alpha} = 0 \\ \epsilon^{ijk}[(\partial_j \mathcal{B}^{\alpha}{}_{k})H'_{\alpha}] - \omega\sqrt{\varepsilon_0\mu_0}\kappa^{ji}\mathcal{B}^{\alpha}{}_{j}H'_{\alpha} = 0 \end{cases} . \tag{B.7}$$

There is a remark that the equations show the transformation matrices are dependent on the $\mathbf{E}$ and $\mathbf{H}$ fields in general. Equation (B.3) becomes

$$\epsilon^{ijk}\mathcal{A}^{\alpha}{}_{k}\partial_j E'_{\alpha} = -i\omega\mu^{ij}\mathcal{B}^{\alpha}{}_{j}H'_{\alpha} \tag{B.8}$$

After repeating the same procedures introduced in above, we can obtain the magnetic tensor in the transformed space,

$$\epsilon^{\gamma\beta\alpha}(\det\boldsymbol{\mathcal{A}})\partial'_{\beta}E'_{\alpha} = -i\omega\mathcal{A}^{\gamma}{}_{i}\mu^{ij}\mathcal{B}^{\alpha}{}_{j}H'_{\alpha} \Rightarrow \ \boldsymbol{\mu}'(\mathbf{x}') = \frac{\boldsymbol{\mathcal{A}}\boldsymbol{\mu}(\mathbf{x})\boldsymbol{\mathcal{B}}^{\boldsymbol{T}}}{\det\boldsymbol{\mathcal{A}}}. \tag{B.9}$$

Similarly, the dielectric permittivity tensor in the transformed space is

$$\boldsymbol{\varepsilon}'(\mathbf{x}') = \frac{\boldsymbol{\mathcal{B}}\boldsymbol{\varepsilon}(\mathbf{x})\boldsymbol{\mathcal{A}}^{\boldsymbol{T}}}{\det\boldsymbol{\mathcal{B}}} \tag{B.10}$$

Note that the transformations (B.9) and (B.10) are reducing the chiral medium to a simple medium, i.e., from complex parameters to simple parameters; however, the normal approach of transformation optics (equation (A.10)) is from simple parameters to complex parameters.

Appendix C

Wave equations in 1D inhomogeneous and anisotropic materials

C.1 Differential matrix equations of 1D isotropic chiral materials

The constitutive relations of isotropic chiral materials are still following linear theories. By supposing EM waves are propagating along z-axis and the time component is harmonic, the macroscopic electric and magnetic fields can be expressed as $\mathbf{E}(\omega, z)e^{-i\omega t}$ and $\mathbf{B}(\omega, z)e^{-i\omega t}$ respectively. Thus, the constitutive relations of 1D

materials can be expressed as

$$\begin{aligned} \mathbf{D}(\omega, z) &= \varepsilon_0 \boldsymbol{\varepsilon}(\omega, z)\mathbf{E}(\omega, z) - i\sqrt{\mu_0 \varepsilon_0}\, \kappa(\omega, z)\mathbf{H}(\omega, z) \\ \mathbf{B}(\omega, z) &= \mu_0 \boldsymbol{\mu}(\omega, z)\mathbf{H}(\omega, z) + i\sqrt{\mu_0 \varepsilon_0}\, \kappa(\omega, z)\mathbf{E}(\omega, z) \end{aligned} . \tag{C.1}$$

On the other hand, Maxwell's equations are

$$\boldsymbol{\nabla} \times \mathbf{E} + i\omega \mathbf{B} = \mathbf{0},\ \boldsymbol{\nabla} \times \mathbf{H} - i\omega \mathbf{D} = \mathbf{0}. \tag{C.2}$$

Thus, Faraday's law can be written as

$$-\frac{d}{dz} \begin{pmatrix} E_y \\ E_x \\ 0 \end{pmatrix} e^{-i\omega t} = i\omega[\mu_0 \boldsymbol{\mu}\mathbf{H} + i\sqrt{\mu_0 \varepsilon_0}\, \kappa \mathbf{E}] e^{-i\omega t}. \tag{C.3}$$

After some mathematical calculation, two sets of equations can be obtained:

$$\frac{d}{dz} \begin{pmatrix} E_x \\ E_y \end{pmatrix} = i\omega\mu_0 \begin{pmatrix} \mu_{21}H_x + \mu_{22}H_y + \mu_{23}H_z \\ -\mu_{11}H_x - \mu_{12}H_y - \mu_{13}H_z \end{pmatrix} - \frac{\omega\kappa}{c} \begin{pmatrix} E_y \\ -E_x \end{pmatrix} \tag{C.4}$$

and

$$H_z + \frac{i\kappa}{\mu_{33}}\sqrt{\frac{\varepsilon_0}{\mu_0}} E_z = -\frac{1}{\mu_{33}}[\mu_{31}H_x + \mu_{32}H_y], \tag{C.5}$$

where c is light speed in vacuum. Similarly, Ampere's law can be written as

$$\frac{d}{dz} \begin{pmatrix} H_x \\ H_y \end{pmatrix} = i\omega\varepsilon_0 \begin{pmatrix} -\varepsilon_{21}E_x - \varepsilon_{22}E_y - \varepsilon_{23}E_z \\ \varepsilon_{11}E_x + \varepsilon_{12}E_y + \varepsilon_{13}E_z \end{pmatrix} + \frac{\omega\kappa}{c} \begin{pmatrix} -H_y \\ H_x \end{pmatrix} \tag{C.6}$$

and

$$H_z - \sqrt{\frac{\varepsilon_0}{\mu_0}}\frac{\varepsilon_{33}}{i\kappa}E_z = \sqrt{\frac{\varepsilon_0}{\mu_0}}\frac{1}{i\kappa}[\varepsilon_{31}E_x + \varepsilon_{32}E_y]. \tag{C.7}$$

By combining equations (C.5) and (C.7) to express E_z and H_z in terms of the x and y components of $\mathbf{E}$ and $\mathbf{H}$ fields, differential matrix equation (2.1) can be obtained after E_z and H_z are substituted into equations (C.4) and (C.6).

C.2 Transformation matrix of 1D isotropic chiral medium and simple medium

Since a mapping between the chiral and simple media is expected, the relation of the wave solution between the virtual and physical spaces should be $\mathbf{F}' = \mathbf{R}\,\mathbf{F} + \mathbf{G}\left(E_z\, E_z\, Z_0 H_z\, Z_0 H_z\right)^T = \boldsymbol{\mathcal{R}}\mathbf{F}$, where transformation matrix $\mathbf{R}(\omega, z) = [[(\boldsymbol{\mathcal{A}}^T)^{-1}]_{ab}] \oplus [[(\boldsymbol{\mathcal{B}}^T)^{-1}]_{ab}]$ $(a, b = 1, 2)$ and $\mathbf{G}(\omega, z)$ is the transformation matrix related to the z-components of EM fields. The symbol $\oplus$ is the direct sum, for example, $\mathbf{A} \oplus \mathbf{B} = \mathrm{diag}(\mathbf{A}, \mathbf{B})$. The most direct way to find out the transformation matrix $\boldsymbol{\mathcal{R}}$ is to solve the differential equation (B.7); fortunately, because of isotropic chirality, matrix calculation is enough to handle this problem instead of tackling the complicated tensor calculation. As the propagation direction of EM waves is parallel to z-axis and the medium are homogeneous in x and y directions, it is not necessary to take the transformation direction different from the propagation direction. As a result, I can immediately say $\mathcal{A}_{13} = \mathcal{A}_{23} = \mathcal{A}_{31} = \mathcal{A}_{32} = 0$ ($\boldsymbol{\mathcal{B}}$ is also the same), so $\boldsymbol{\mathcal{R}} = \mathbf{R}$. The differential matrices in two spaces are

$$\frac{d}{dz}\mathbf{F}(\omega, z) = \frac{i\omega}{c}\Big[\mathbf{M}(\omega, z) + i\mathbf{K}(\omega, z) + \mathbf{L}(\omega, z)\Big]\mathbf{F}(\omega, z), \tag{C.8}$$

and

$$\frac{d}{dz'}\mathbf{F}'(\omega,z') = \frac{i\omega}{c}\Big[\mathbf{M}'(\omega,z') + \mathbf{L}'(\omega,z')\Big]\mathbf{F}'(\omega,z'). \tag{C.9}$$

By substituting the relation of solutions into (C.8), the equation becomes

$$\Big[\frac{d}{dz}\mathbf{R}^{-1}(z)\Big]\mathbf{F}'(z') + \mathbf{R}^{-1}(z)\Big[\frac{d}{dz}\mathbf{F}'(z')\Big] = \frac{i\omega}{c}\Big[\mathbf{M}(z) + i\mathbf{K}(z) + \mathbf{L}(z)\Big]\mathbf{R}^{-1}(z)\mathbf{F}'(z'),$$

where ω is omitted in this step. According to equation (2.4), $\mathbf{L}$ can be further expressed as $\mathbf{L} = \mathbf{L_1} + i\mathbf{L_2}$, where $\mathbf{L_1}$ is an anti-block diagonal matrix and $\mathbf{L_2}$ is a block diagonal matrix. The differential matrix equation can be expressed as

$$\begin{aligned}\frac{d}{dz}\mathbf{F}'(z) = \Big[&\frac{i\omega}{c}\mathbf{R}(z)\Big(\mathbf{M}(z) + \mathbf{L_1}(z)\Big)\mathbf{R}^{-1}(z) \\ &- \Big(\frac{\omega}{c}\mathbf{R}(z)\Big(\mathbf{K}(z) + \mathbf{L_2}(z)\Big)\mathbf{R}^{-1}(z) + \mathbf{R}(z)\Big[\frac{d}{dz}\mathbf{R}^{-1}(z)\Big]\Big)\Big]\mathbf{F}'(z).\end{aligned} \tag{C.10}$$

By comparing equations (C.8) to (C.9), the block diagonal matrices are related to the chirality, which should be eliminated during the transformation. If I further assume the space is independent of x and y components of EM fields, the second term in the square bracket vanishes. Thus,

$$\frac{d}{dz}\begin{pmatrix}\mathcal{A}_{11}\\ \mathcal{A}_{12}\\ \mathcal{A}_{21}\\ \mathcal{A}_{22}\end{pmatrix} = -\frac{\omega}{c}\kappa\mathbf{I}_{2\times2}\otimes\begin{pmatrix}\frac{\mu_{23}\varepsilon_{31}}{\varepsilon_{33}\mu_{33}-\kappa^2} & 1+\frac{\mu_{23}\varepsilon_{32}}{\varepsilon_{33}\mu_{33}-\kappa^2}\\ -(1+\frac{\mu_{13}\varepsilon_{31}}{\varepsilon_{33}\mu_{33}-\kappa^2}) & -\frac{\mu_{13}\varepsilon_{32}}{\varepsilon_{33}\mu_{33}-\kappa^2}\end{pmatrix}\begin{pmatrix}\mathcal{A}_{11}\\ \mathcal{A}_{12}\\ \mathcal{A}_{21}\\ \mathcal{A}_{22}\end{pmatrix}, \tag{C.11}$$

where $\mathbf{I}$ is an identity matrix. The system of differential equations of $\boldsymbol{\mathcal{B}}_{ab}$ is similar but interchanging μ and ε. There is no analytical solution of equation (C.11) in

general. If $\mu_{31} = \mu_{32} = \mu_{13} = \mu_{23} = 0$, equation (C.11) will be

$$\frac{d}{dz}\begin{pmatrix} \mathcal{A}_{11} \\ \mathcal{A}_{12} \\ \mathcal{A}_{21} \\ \mathcal{A}_{22} \end{pmatrix} = \frac{\omega}{c}\kappa \begin{pmatrix} 0 & -1 & 0 & 0 \\ 1 & 0 & 0 & 0 \\ 0 & 0 & 0 & -1 \\ 0 & 0 & 1 & 0 \end{pmatrix} \begin{pmatrix} \mathcal{A}_{11} \\ \mathcal{A}_{12} \\ \mathcal{A}_{21} \\ \mathcal{A}_{22} \end{pmatrix}. \tag{C.12}$$

The transformation of **E** and **H** fields are the same, i.e., $\boldsymbol{\mathcal{A}} = \boldsymbol{\mathcal{B}}$, so the transformation matrix will be denoted as **A**. After the above systems of differential equations have been solved and applied the condition of fixed surface, $\mathbf{A}(z_0) = \mathbf{I}$, we can get

$$[\mathbf{A}_{ab}] = \begin{pmatrix} \cos\theta & \sin\theta \\ -\sin\theta & \cos\theta \end{pmatrix}, \tag{C.13}$$

where

$$\theta(\omega, z) = \frac{\omega}{c}\int_{z_0}^{z} \kappa(\omega, u)\, du. \tag{C.14}$$

On the other hand, the remained parts in equation (C.10) are related to the tensors in the transformed space. The transformation of differential operator is $\partial_j = A^{\beta}{}_{j}\partial'_{\beta} \Rightarrow d/dz = A_{33}(d/dz')$. Equation (C.10) becomes

$$\frac{d}{dz'}\mathbf{F}'(z') = \frac{1}{A_{33}}\Big[\frac{i\omega}{c}\mathbf{R}(z)\Big(\mathbf{M}(z) + \mathbf{L_1}(z)\Big)\mathbf{R}^{-1}(z)\Big]\mathbf{F}'(z'). \tag{C.15}$$

As the transformations of dielectric and magnetic tensors should follow equations (B.10) and (B.9) respectively. i.e.

$$\boldsymbol{\varepsilon}'(\mathbf{x}') = \frac{\mathbf{A}\boldsymbol{\varepsilon}(\mathbf{x})\mathbf{A}^T}{\det\mathbf{A}}$$
$$= \begin{pmatrix} \frac{\varepsilon_{11}(A_{11})^2+(\varepsilon_{12}+\varepsilon_{21})A_{11}A_{12}+\varepsilon_{22}(A_{12})^2}{A_{33}} & \frac{\varepsilon_{12}(A_{11})^2-(\varepsilon_{11}-\varepsilon_{22})A_{11}A_{12}-\varepsilon_{21}(A_{12})^2}{A_{33}} & \varepsilon_{13}A_{11}+\varepsilon_{23}A_{12} \\ \frac{\varepsilon_{21}(A_{11})^2-(\varepsilon_{11}-\varepsilon_{22})A_{11}A_{12}-\varepsilon_{12}(A_{12})^2}{A_{33}} & \frac{\varepsilon_{22}(A_{11})^2-(\varepsilon_{12}+\varepsilon_{21})A_{11}A_{12}+\varepsilon_{11}(A_{12})^2}{A_{33}} & \varepsilon_{23}A_{11}-\varepsilon_{13}A_{12} \\ \varepsilon_{31}A_{11}+\varepsilon_{32}A_{12} & \varepsilon_{32}A_{11}-\varepsilon_{31}A_{12} & \varepsilon_{33}A_{33} \end{pmatrix}, \tag{C.16}$$

where $A_{21} = -A_{12}$, $A_{11} = A_{22}$ and $(A_{11})^2 + (A_{22})^2 = 1$. Again, the magnetic tensor can be found by replacing ε to μ. After comparing the terms in equation (C.9) one by one, it is not difficult to notice they match with (C.16) except ε'_{33} and μ'_{33}. i.e.,

$$\begin{cases} \varepsilon'_{33} = A_{33}(\varepsilon_{33} - \frac{\kappa^2}{\mu_{33}}) \\ \mu'_{33} = A_{33}(\mu_{33} - \frac{\kappa^2}{\varepsilon_{33}}) \end{cases}. \tag{C.17}$$

It seems contradicting with (C.16); the reason can be contributed to the transformation limited in the form of (B.6). However, this contradiction can be resolved if a gradient of scalar fields are inserted in the transformation. i.e., $\mathbf{E} = \boldsymbol{\mathcal{A}}^T(\mathbf{E}' - \nabla'\phi)$ and $\mathbf{H} = \boldsymbol{\mathcal{B}}^T(\mathbf{H}' - \nabla'\psi)$, the electric and magnetic tensors in the virtual space become

$$\boldsymbol{\varepsilon}'(\mathbf{x}') \to \boldsymbol{\varepsilon}'(\mathbf{x}') + \boldsymbol{\Delta\varepsilon}'(\mathbf{x}') \text{ and } \boldsymbol{\mu}'(\mathbf{x}') \to \boldsymbol{\mu}'(\mathbf{x}') + \boldsymbol{\Delta\mu}'(\mathbf{x}'), \tag{C.18}$$

where

$$\Delta\varepsilon'_{33} = -A_{33}\frac{\kappa^2}{\mu_{33}}, \ \Delta\mu'_{33} = -A_{33}\frac{\kappa^2}{\varepsilon_{33}} \tag{C.19}$$

and the other elements are all equal to 0 in this situation. The analogy of inserted scalar fields is difficult, which can even be extended to another research topic. Here, I will not cover the details here. In this study, diagonal permittivity and permeability tensors in the virtual space are chosen, which results in $\mathbf{L} = \mathbf{0}$ such that this problem can be neglected.

Appendix D

Properties of the dispersion relations of the chiral photonic crystals

The dispersion relation of the original chiral photonic crystal can be found by equation (2.12). By supposing $\phi(a) = \theta(a) - \pi$, where $\theta(a) \in [\pi, 2\pi)$, the dispersion relation is

$$\begin{aligned} e^{iv\pi}\mathbf{F}(\omega, 0) &= \mathbf{R}^{-1}\big(\theta(a)\big)\exp\Big(\frac{i\omega a}{c}\mathbf{M}'\Big)\mathbf{F}(\omega, 0) \\ &= -\mathbf{R}^{-1}\big(\phi(a)\big)\exp\Big(\frac{i\omega a}{c}\mathbf{M}'\Big)\mathbf{F}(\omega, 0) \\ &= e^{i(u\pm 1)\pi}\mathbf{F}(\omega, 0), \end{aligned}$$

where v and u are the normalized Bloch's vector when the structural "twisted" angles are $\theta(a)$ and $\phi(a)$ respectively. It is clear that the band structure of $\theta(a)$ can overlap with the band structure of $\phi(a)$ by shifting either one to the left (or right) by 1; also the eigenvectors follow the shifting. The similar results can be found in the

region $[0, \pi/2)$ and $[\pi/2, \pi)$; nevertheless, the eigenvectors do not follow the shifting. Let $\phi(a) = \pi - \theta(a)$, where $\theta(a) \in (\pi/2, \pi]$. The dispersion relation is

$$\begin{aligned} e^{iv\pi}\mathbf{F}(\omega, 0) &= \mathbf{R}^{-1}\big(\theta(a)\big)\exp\Big(\frac{i\omega a}{c}\mathbf{M}'\Big)\mathbf{F}(\omega, 0) \\ &= -\mathbf{R}\big(\phi(a)\big)\exp\Big(\frac{i\omega a}{c}\mathbf{M}'\Big)\mathbf{F}(\omega, 0) \\ &\neq -\mathbf{R}^{-1}\big(\phi(a)\big)\exp\Big(\frac{i\omega a}{c}\mathbf{M}'\Big)\mathbf{F}(\omega, 0) \\ &= e^{i(u\pm 1)\pi}\mathbf{F}(\omega, 0). \end{aligned}$$

Although the results do show the normalized Bloch vectors $u \pm 1$ equals v, this cannot ensure the eigenvectors are the same. Therefore, the region $\theta(a) \in [0, \pi]$ is mainly considered in this study.

Appendix E

Dispersion relations and Zak phases calculated by choosing different origins

By Bloch's theorem, the dispersion relation of the designed chiral photonic crystal is

$$\mathbf{R}^{-1}(a)\exp\Big(\frac{i\omega a}{c}\mathbf{M}'\Big)\mathbf{F}(\omega,0)=e^{ik_z a}\mathbf{F}(\omega,0), \tag{E.1}$$

where the dielectric and magnetic tensors in the virtual space are supposed to be $\mathrm{diag}(\varepsilon'_{11},\varepsilon'_{22},\varepsilon'_{33})$ and $\mathrm{diag}(\mu'_{11},\mu'_{22},\mu'_{33})$. The dispersion relation and eigenstates only depend on $\theta(a)$ if the frequency and electromagnetic tensors in the virtual space are fixed. In other words, no matter what functions $\theta(z)$ they are, the band structures and eigenstates are the same if $\theta(a)$ are the same. In chapter 2, constant chirality is chosen due to convenience, whereas it can be any functions of z in general. Thus,

$\theta(z)$ in a unit cell should be expressed as

$$\theta(z) = \theta_{max} f(z). \tag{E.2}$$

where $f(z)$ is an arbitrary function and its maximum is 1. As mentioned in chapter 1, the eigenstates and Zak phases of isolated bands are dependent on the choice of origin. The dispersion relation has to be modified when different origins are chosen. The modified equation is

$$e^{ik_z a}\mathbf{F}(\omega,0) = \mathbf{R}^{-1}(a)\exp\Big(\frac{i\omega a}{c}\big(1-\frac{d}{a}\big)\mathbf{M}'\Big)\mathbf{R}^{-1}(d)\exp\Big(\frac{i\omega a}{c}\big(\frac{d}{a}\big)\mathbf{M}'\Big)\mathbf{R}(0)\mathbf{F}(\omega,0), \tag{E.3}$$

where d is the distance from the origin to the position that $\theta(z)$ reaches its maximum value. i.e., $f(d) = 1$. Due to $\mathbf{R}(a) = \mathbf{R}(0)$, the dispersion relation can be further expressed as

$$e^{ik_z a}\mathbf{G}(\omega,0) = \exp\Big(\frac{i\omega a}{c}\big(1-\frac{d}{a}\big)\mathbf{M}'\Big)\mathbf{R}^{-1}(d)\exp\Big(\frac{i\omega a}{c}\big(\frac{d}{a}\big)\mathbf{M}'\Big)\mathbf{G}(\omega,0), \tag{E.4}$$

where $\mathbf{G}(\omega,0) = \mathbf{R}^{-1}(0)\mathbf{F}(\omega,0)$. It is clear that the eigenvalues of equations (E.3) and (E.4) are equivalent. Zak phase of an isolated band can be calculated numerically by

$$\Phi_n^{\text{Zak}} = i\sum_m \ln(F_m^\dagger\, F_{m+1}) + i\,\ln(F_f^\dagger\, F_i), \tag{E.5}$$

where F_m is the normalized eigenstate at the mth Bloch wave vector $k_{z,m}$. Owing to the relation $\mathbf{G}(\omega,0) = \mathbf{R}^{-1}(0)\mathbf{F}(\omega,0)$ and $\mathbf{R}^{-1}(0) = \mathbf{R}^\dagger(0)$, the Zak phases calculated by $\mathbf{F}$ and $\mathbf{G}$ are equivalent. As a result, the value of $\theta(0)$, which is

related to the choices of origin, will not affect the band structure and the values of Zak phases.

Appendix F

Separating two modes of the transformed photonic crystals

F.1 Electromagnetic tensors in the transformed structures

According to equation (C.10), the transformation is according to following relation:

$$\frac{d}{dz}\mathbf{F}''(z) = \Big[\frac{i\omega}{c}\mathbf{R}(z)\Big(\mathbf{M}(z)+\mathbf{L_1}(z)\Big)\mathbf{R}^{-1}(z) - \Big(\frac{\omega}{c}\mathbf{R}(z)\Big(\mathbf{K}(z)+\mathbf{L_2}(z)\Big)\mathbf{R}^{-1}(z)+\mathbf{R}(z)\Big[\frac{d}{dz}\mathbf{R}^{-1}(z)\Big]\Big)\Big]\mathbf{F}''(z), \tag{F.1}$$

where ω is omitted in this step due to tidiness. $\mathbf{R}(z)$ is a continuous transformation matrix here because $\theta(z)$ is replaced by $\phi(z)$. The second term in the square bracket on the right hand side is contributed by the chirality. By choos-

ing $\boldsymbol{\varepsilon}' = \text{diag}(\varepsilon'_{11}, \varepsilon'_{22}, \varepsilon'_{33})$ and $\boldsymbol{\mu}' = \text{diag}(\mu'_{11}, \mu'_{22}, \mu'_{33})$, the chirality parameter in the transformed structure is

$$\kappa'' = \frac{d\phi}{dz} - \frac{\omega}{c}\kappa(\omega, z) = \frac{d\phi}{dz} - \frac{\theta_{max}}{a},$$

where $\theta_{max} = \theta(a)$. Because of $\phi(z) = \theta_{max} z/a$ according to the lemma (2.14), the above equation becomes

$$\kappa'' = \frac{d\phi}{dz} - \frac{\theta_{max}}{a} = 0. \tag{F.2}$$

Therefore, the chirality returns to zero in the transformed structure. The remaining parts in equation (F.1) stands for the dielectric and magnetic parameters in the transformed structure, which are expressed in equation (3.4) if $\theta(a) = \pi/2$ is chosen. The proof is trivial and omitted.

F.2 Dispersion relation of the transformed structure

The structural "twisted" angle $\theta(a)$ equal to $\pi/2$ is mainly considered in this study since there is the largest number of complete photonic band gaps. Again, the permittivity and permeability tensors in the virtual space are supposed to be $\text{diag}(\varepsilon'_{11}, \varepsilon'_{22}, \varepsilon'_{33})$ and $\text{diag}(\mu'_{11}, \mu'_{22}, \mu'_{33})$ so that $\mathbf{L}(z) = \mathbf{0}$. The transformed structure is a simple anisotropic binary photonic crystal, which is shown in Fig. 3.4, where the permittivity and permeability tensors are expressed in equation (3.4). If $\mathbf{F}''$ is rearranged in the form $\left(E''_{x''}\ Z_0 H''_{y''}\ E''_{y''}\ -Z_0 H''_{x''}\right)^T = \left(|\psi_{x''}\rangle\ |\psi_{y''}\rangle\right)^T$ and the white and black slabs are named as A and B slabs respectively (where w and b are used

in chapter 3), the matrices $\mathbf{M}''$ of two slabs are

$$\mathbf{M}''_A = \begin{pmatrix} 0 & \mu'_{22} & 0 & 0 \\ \varepsilon'_{11} & 0 & 0 & 0 \\ 0 & 0 & 0 & \mu'_{11} \\ 0 & 0 & \varepsilon'_{22} & 0 \end{pmatrix} \equiv \mathbf{X} \oplus \mathbf{Y} \tag{F.3}$$

and

$$\mathbf{M}''_B = \begin{pmatrix} 0 & \mu'_{11} & 0 & 0 \\ \varepsilon'_{22} & 0 & 0 & 0 \\ 0 & 0 & 0 & \mu'_{22} \\ 0 & 0 & \varepsilon'_{11} & 0 \end{pmatrix} \equiv \mathbf{Y} \oplus \mathbf{X}. \tag{F.4}$$

$|\psi_{x''}\rangle$ and $|\psi_{y''}\rangle$ can be considered individually because the operator is block-diagonal now. The dispersion relations of $|\psi_{x''}\rangle$ and $|\psi_{y''}\rangle$ modes are

$$\begin{cases} e^{ik''_z\Lambda}|\psi_{x''}\rangle = \exp\Big(\dfrac{i\omega a}{c}\mathbf{Y}\Big)\exp\Big(\dfrac{i\omega a}{c}\mathbf{X}\Big)|\psi_{x''}\rangle \\ e^{ik''_z\Lambda}|\psi_{y''}\rangle = \exp\Big(\dfrac{i\omega a}{c}\mathbf{X}\Big)\exp\Big(\dfrac{i\omega a}{c}\mathbf{Y}\Big)|\psi_{y''}\rangle \end{cases}. \tag{F.5}$$

There is a remark that the matrices $\mathbf{M}$ in isotropic binary photonic crystals are $\mathbf{M}_A = \mathbf{X} \oplus \mathbf{X}$ and $\mathbf{M}_B = \mathbf{Y} \oplus \mathbf{Y}$ so the eigenvectors of $|\psi_x\rangle$ and $|\psi_y\rangle$ are the same. From equations (F.3) and (F.4), the structure can be regarded as XY and YX isotropic layered structures if $|\psi_{x''}\rangle$ and $|\psi_{y''}\rangle$ are individually considered respectively. Even though the dispersion relations of $|\psi_{x''}\rangle$ and $|\psi_{y''}\rangle$ modes are the same, the eigenvectors of the same isolated band are different.

F.3 Relation of the Bloch vectors in two structures

In the original chiral photonic crystal, the dispersion relation can be found by equation (2.13). If the eigenvector rearranged in the form $\mathbf{F} = \big(|\psi_x\rangle\ |\psi_y\rangle\big)^T$, the operator can be expressed as

$$\mathbf{R}^{-1}(\theta)\exp\Big(\frac{i\omega a}{c}\mathbf{M}'\Big) = \Bigg[\mathbf{I}_{2\times 2}\otimes \begin{pmatrix}\cos\theta & -\sin\theta\\ \sin\theta & \cos\theta\end{pmatrix}\Bigg]\exp\Big(\frac{i\omega a}{c}\big(\mathbf{X}\oplus\mathbf{Y}\big)\Big). \quad \text{(F.6)}$$

The dispersion relations of $|\psi_x\rangle$ and $|\psi_y\rangle$ modes are

$$\begin{cases} e^{ik_z a}|\psi_x\rangle = \cos\theta\exp\Big(\frac{i\omega a}{c}\mathbf{X}\Big)|\psi_x\rangle - \sin\theta\exp\Big(\frac{i\omega a}{c}\mathbf{Y}\Big)|\psi_y\rangle \\ e^{ik_z a}|\psi_y\rangle = \sin\theta\exp\Big(\frac{i\omega a}{c}\mathbf{X}\Big)|\psi_x\rangle + \cos\theta\exp\Big(\frac{i\omega a}{c}\mathbf{Y}\Big)|\psi_y\rangle \end{cases}. \quad \text{(F.7)}$$

Furthermore, when $\theta(a) = \pi/2$, the dispersion relation can be simplified as

$$\begin{cases} e^{2ik_z a}|\psi_x\rangle = -\exp\Big(\frac{i\omega a}{c}\mathbf{Y}\Big)\exp\Big(\frac{i\omega a}{c}\mathbf{X}\Big)|\psi_x\rangle \\ e^{2ik_z a}|\psi_y\rangle = -\exp\Big(\frac{i\omega a}{c}\mathbf{X}\Big)\exp\Big(\frac{i\omega a}{c}\mathbf{Y}\Big)|\psi_y\rangle \end{cases}$$

$$\Rightarrow \begin{cases} e^{2ik_z a\pm\pi}|\psi_x\rangle = \exp\Big(\frac{i\omega a}{c}\mathbf{Y}\Big)\exp\Big(\frac{i\omega a}{c}\mathbf{X}\Big)|\psi_x\rangle \\ e^{2ik_z a\pm\pi}|\psi_y\rangle = \exp\Big(\frac{i\omega a}{c}\mathbf{X}\Big)\exp\Big(\frac{i\omega a}{c}\mathbf{Y}\Big)|\psi_y\rangle \end{cases}. \quad \text{(F.8)}$$

Therefore, the eigenvectors $|\psi_x(k_z\Lambda/\pi \pm 1)\rangle$ and $|\psi_y(k_z\Lambda/\pi \pm 1)\rangle$ equal $|\psi_{x''}(k_z'')\rangle$ and $|\psi_{y''}(k_z'')\rangle$ respectively, and the relation of the eigenvalue is

$$\frac{k_z\Lambda}{\pi} = \frac{k_z''\Lambda}{\pi} + (2s-1), \tag{F.9}$$

where $\Lambda = 2a$ and s is an integer for controlling the normalized wave vector within the range of -1 and 1.

References

[1] J. B. Pendry, D. Schurig, and D. R. Smith. Controlling electromagnetic fields. *Science*, 312(5781):1780–1782, 2006.

[2] Ulf Leonhardt. Optical conformal mapping. *Science*, 312(5781):1777–1780, 2006.

[3] Yun Lai, Jack Ng, and C.T. Chan. Creating illusion effects using transformation optics. *Transformation Electromagnetics and Metamaterials: Fundamental Principles and Applications*, pages 139–165, 07 2013.

[4] Huanyang Chen, Che Ting Chan, and Ping Sheng. Transformation optics and metamaterials. *Nature materials*, 9(5):387–396, 2010.

[5] Do-Hoon Kwon and Douglas H. Werner. Polarization splitter and polarization rotator designs based on transformation optics. *Opt. Express*, 16(23):18731–18738, Nov 2008.

[6] Paloma A Huidobro, Maxim L Nesterov, Luis Martín-Moreno, and Francisco J García-Vidal. Transformation optics for plasmonics. *Nano letters*, 10(6):1985–1990, 2010.

[7] Douglas H Werner and Do-Hoon Kwon. *Transformation electromagnetics and metamaterials*. Springer, 2013.

[8] Yongliang Zhang, Lina Shi, Ruo-Yang Zhang, Jinglai Duan, Jack Ng, C. T. Chan, and Kin Hung Fung. Metric-torsion duality of optically chiral structures. *Phys. Rev. Lett.*, 122:200201, May 2019.

[9] A. H. Sihvola, A. J. Viitanen, I. V. Lindell, and S. A. Tretyakov. *Electromagnetic Waves in Chiral and Bi-Isotropic Media*. Artech House Antenna Library, Norwood, MA, 1994.

[10] Ling Lu, John D Joannopoulos, and Marin Soljačić. Topological photonics. *Nature photonics*, 8(11):821–829, 2014.

[11] S. Raghu and F. D. M. Haldane. Analogs of quantum-hall-effect edge states in photonic crystals. *Phys. Rev. A*, 78:033834, Sep 2008.

[12] Zheng Wang, Y. D. Chong, John D. Joannopoulos, and Marin Soljačić. Reflection-free one-way edge modes in a gyromagnetic photonic crystal. *Phys. Rev. Lett.*, 100:013905, Jan 2008.

[13] Wen-Jie Chen, Shao-Ji Jiang, Xiao-Dong Chen, Baocheng Zhu, Lei Zhou, Jian-Wen Dong, and Che Ting Chan. Experimental realization of photonic topological insulator in a uniaxial metacrystal waveguide. *Nature communications*, 5(1):1–7, 2014.

[14] Ling Lu, John D Joannopoulos, and Marin Soljačić. Topological states in photonic systems. *Nature Physics*, 12(7):626–629, 2016.

[15] Qiang Wang, Meng Xiao, Hui Liu, Shining Zhu, and C. T. Chan. Measurement of the zak phase of photonic bands through the interface states of a metasurface/photonic crystal. *Phys. Rev. B*, 93:041415, Jan 2016.

[16] Martin Esmann, Fabrice Roland Lamberti, Pascale Senellart, Ivan Favero, Olivier Krebs, Loïc Lanco, Carmen Gomez Carbonell, Aristide Lemaître, and Norberto Daniel Lanzillotti-Kimura. Topological nanophononic states by band inversion. *Phys. Rev. B*, 97:155422, Apr 2018.

[17] Aaswath Raman and Shanhui Fan. Photonic band structure of dispersive metamaterials formulated as a hermitian eigenvalue problem. *Phys. Rev. Lett.*, 104:087401, Feb 2010.

[18] You-Zhong Yu, Chih-Yu Kuo, Ruey-Lin Chern, and Che Ting Chan. Photonic topological semimetals in bianisotropic metamaterials. *Scientific Reports*, 9(1):1–13, 2019.

[19] Alexander B Khanikaev, S Hossein Mousavi, Wang-Kong Tse, Mehdi Kargarian, Allan H MacDonald, and Gennady Shvets. Photonic topological insulators. *Nature materials*, 12(3):233–239, 2013.

[20] Sotiris Droulias, Ioannis Katsantonis, Maria Kafesaki, Costas M. Soukoulis, and Eleftherios N. Economou. Chiral metamaterials with *pt* symmetry and beyond. *Phys. Rev. Lett.*, 122:213201, May 2019.

[21] Meng Xiao, Qian Lin, and Shanhui Fan. Hyperbolic weyl point in reciprocal chiral metamaterials. *Phys. Rev. Lett.*, 117:057401, Jul 2016.

[22] Wenlong Gao, Mark Lawrence, Biao Yang, Fu Liu, Fengzhou Fang, Benjamin

Béri, Jensen Li, and Shuang Zhang. Topological photonic phase in chiral hyperbolic metamaterials. *Phys. Rev. Lett.*, 114:037402, Jan 2015.

[23] Bingnan Wang, Jiangfeng Zhou, Thomas Koschny, Maria Kafesaki, and Costas M Soukoulis. Chiral metamaterials: simulations and experiments. *Journal of Optics A: Pure and Applied Optics*, 11(11):114003, sep 2009.

[24] Jungho Mun, Minkyung Kim, Younghwan Yang, Trevon Badloe, Jincheng Ni, Yang Chen, Cheng-Wei Qiu, and Junsuk Rho. Electromagnetic chirality: from fundamentals to nontraditional chiroptical phenomena. *Light: Science & Applications*, 9(1):1–18, 2020.

[25] L.D. Barron. True and false chirality and parity violation. *Chemical Physics Letters*, 123(5):423 – 427, 1986.

[26] SA Tretyakov, AH Sihvola, AA Sochava, and CR Simovski. Magnetoelectric interactions in bi-anisotropic media. *Journal of Electromagnetic Waves and Applications*, 12(4):481–497, 1998.

[27] Tom G Mackay and Akhlesh Lakhtakia. *Electromagnetic Anisotropy and Bianisotropy*. WORLD SCIENTIFIC, 2009.

[28] Kin Hung Fung, Jeffrey Chi Wai Lee, and Che Ting Chan. *CHIRAL PHOTONIC AND PLASMONIC STRUCTURES*. World Scientific, 2011.

[29] Jiangfeng Zhou, Jianfeng Dong, Bingnan Wang, Thomas Koschny, Maria Kafesaki, and Costas M. Soukoulis. Negative refractive index due to chirality. *Phys. Rev. B*, 79:121104, Mar 2009.

[30] Hanju Rhee, Young-Gun June, Jang-Soo Lee, Kyung-Koo Lee, Jeong-Hyon Ha, Zee Hwan Kim, Seung-Joon Jeon, and Minhaeng Cho. Femtosecond characterization of vibrational optical activity of chiral molecules. *Nature*, 458(7236):310–313, 2009.

[31] Michael Victor Berry. Quantal phase factors accompanying adiabatic changes. *Proceedings of the Royal Society of London. A. Mathematical and Physical Sciences*, 392(1802):45–57, 1984.

[32] J. J. Sakurai and Jim Napolitano. *Modern Quantum Mechanics*. Cambridge University Press, 2 edition, 2017.

[33] J. Zak. Berry's phase for energy bands in solids. *Phys. Rev. Lett.*, 62:2747–2750, Jun 1989.

[34] Raffaele Resta. Manifestations of berry' s phase in molecules and condensed matter. *Journal of Physics: Condensed Matter*, 12(9):R107–R143, feb 2000.

[35] Meng Xiao, Z. Q. Zhang, and C. T. Chan. Surface impedance and bulk band geometric phases in one-dimensional systems. *Phys. Rev. X*, 4:021017, Apr 2014.

[36] Ka Hei Choi, C. W. Ling, K. F. Lee, Y. H. Tsang, and Kin Hung Fung. Simultaneous multi-frequency topological edge modes between one-dimensional photonic crystals. *Opt. Lett.*, 41(7):1644–1647, Apr 2016.

[37] Nicholas J Bianchi and Leonard M Kahn. Optical states in a 1d superlattice with multiple photonic crystal interfaces. *Journal of Optics*, 22(6):065101, may 2020.

[38] C. W. Oseen. The theory of liquid crystals. *Transactions of the Faraday Society*, 29(140):883–899, 1933.

[39] Ion Bita and Edwin L. Thomas. Structurally chiral photonic crystals with magneto-optic activity: indirect photonic bandgaps, negative refraction, and superprism effects. *J. Opt. Soc. Am. B*, 22(6):1199–1210, Jun 2005.